The Innovation

Review

Artificial Structural Colors and Applications

Zhiyi Xuan,[1,3,4,5,7] Junyu Li,[2,7] Qingquan Liu,[1,3,4,5] Fei Yi,[2] Shaowei Wang,[1,3,4,6,*] and Wei Lu[1,3,4,5,6]
*Correspondence: wangshw@mail.sitp.ac.cn
Received: August 8, 2020; Accepted: January 13, 2021; Published Online: January 18, 2021; https://doi.org/10.1016/j.xinn.2021.100081

GRAPHICAL ABSTRACT

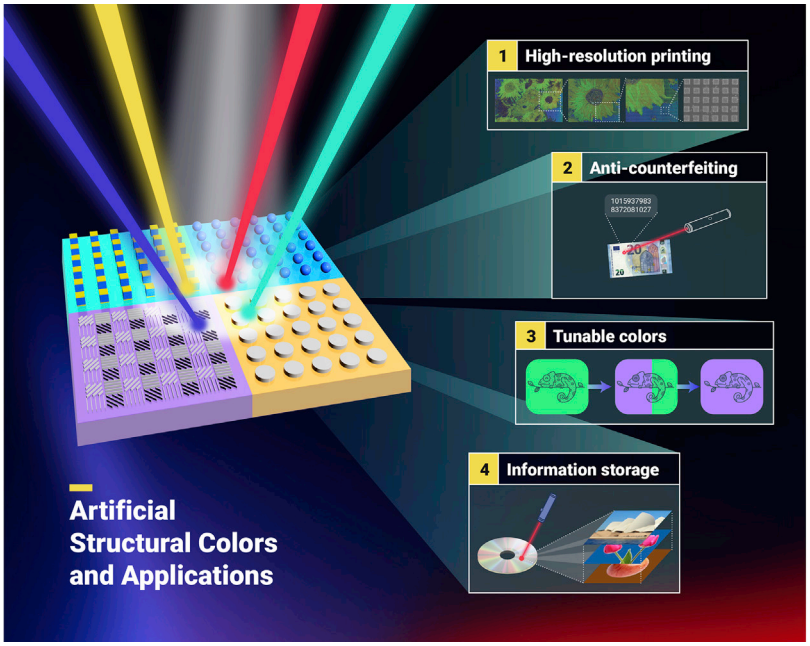

PUBLIC SUMMARY

- Structural colors are colors generated by the interaction between incident light and nanostructures
- High-resolution and long-term stable structural colors, can be designed as functional devices
- Structural colors have application prospects in many fields, such as high-resolution printing and anti-counterfeiting

Review

Artificial Structural Colors and Applications

Zhiyi Xuan,[1,3,4,5,7] Junyu Li,[2,7] Qingquan Liu,[1,3,4,5] Fei Yi,[2] Shaowei Wang,[1,3,4,6,*] and Wei Lu[1,3,4,5,6]

[1]State Key Laboratory of Infrared Physics, Shanghai Institute of Technical Physics, Chinese Academy of Sciences, Shanghai 200083, China

[2]School of Optical and Electronic Information, Huazhong University of Science and Technology, Wuhan 430074, China

[3]Shanghai Engineering Research Center of Energy-saving Coatings, Shanghai 200083, China

[4]University of Chinese Academy of Sciences, Beijing, 100049, China

[5]School of Physical Science and Technology, ShanghaiTech University, Shanghai 201210, China

[6]Shanghai Research Center for Quantum Sciences, Shanghai 201315, China

[7]These authors contributed equally

*Correspondence: wangshw@mail.sitp.ac.cn

Received: August 8, 2020; Accepted: January 13, 2021; Published Online: January 18, 2021; https://doi.org/10.1016/j.xinn.2021.100081

Citation: Xuan Z., Li J., Liu J., et al. (2021). Artificial structural colors and applications. The Innovation **2(1)**, 100081.

Structural colors are colors generated by the interaction between incident light and nanostructures. Structural colors have been studied for decades due to their promising advantages of long-term stability and environmentally friendly properties compared with conventional pigments and dyes. Previous studies have demonstrated many artificial structural colors inspired by naturally generated colors from plants and animals. Moreover, many strategies consisting of different principles have been reported to achieve dynamically tunable structural colors. Furthermore, the artificial structural colors can have multiple functions besides decoration, such as absorbing solar energy, anti-counterfeiting, and information encryption. In the present work, we reviewed the typical artificial structural colors generated by multilayer films, photonic crystals, and metasurfaces according to the type of structures, and discussed the approaches to achieve dynamically tunable structural colors.

INTRODUCTION

Color is the visual perception of light produced by the eyes, brain, and life experience. The light we see with naked eyes is generated by electromagnetic waves within a visible light range. The optic nerve sensation is caused by the naked eyes stimulated by electromagnetic radiation, leading to the difference in colors. When the visible light irradiates on matter, it can be reflected and transmitted, while some of it is absorbed. Therefore, different colors are generated, bringing us a colorful world. Pigments, bioluminescence, and structural colors are the three primary sources of color in nature. Traditionally, pigments and dyes are used to make objects showing beautiful colors. The application of pigments is well-known and extensively used in our daily lives. Although the traditional dyeing approach dramatically facilitates human beings' lives, it also has obvious shortcomings, such as non-recyclability and environmental pollution. Due to the instability of chemicals, the color produced by dyes or pigments lacks durability. In contrast, structural coloration possesses many advantages, such as long-term stability, sustainable production, and even having multi-functions, which is environmentally friendly and dynamically tunable.

The structural color has been studied for a long time. Hooke[1] and Newton[2] described the microstructure of silverfish and the brilliant feathers of peacocks, respectively. Later, the invention of the electron microscope helped people study the colors at the micrometer scale. The periodic structures of opals, sea mouse, and many other animals have gradually been investigated.[3] In 2003, Jian Zi et al.[4] revealed the physical mechanism underlying the brilliant colors of peacock feathers, sparking the researchers' great interest in structural colors. Because of the excellent performance of structural colors, researchers have carried out many biomimetic investigations of natural structural colors.[5–8] Animals such as chameleon and octopus can dynamically adjust their surface colors,[9–11] which has also inspired researchers to demonstrate dynamically tunable structural colors.

The nanostructure generates colors via different structural geometries,[12–19] and involves the tuning of resonance light within the visible wavelength range via manipulating structural parameters.[20–24] The fast development of nanofabrication technologies leads to the creation of artificial resonances and exotic light-matter interactions.[25–29] It opens new ways for the production of novel structures, such as multilayer films, photonic crystals, and metasurfaces.[30–37] Many subwavelength structural colors have been demonstrated with a resolution beyond the diffraction limit,[32,38–41] which benefits from the sub-diffraction localization of light. Besides, based on proven digital imaging techniques, primary color components (red, green, blue or cyan, magenta, and yellow)[42] can be precisely balanced in each pixel, thereby realizing structural color printing with high resolution.[43] Moreover, the type of material plays a crucial role in color generation. For example, the structure of all-dielectric elements with resonance and scattering effect can make a narrowband spectrum, enhancing the color contrast over the whole visible range.[30,35,44–48] However, metal structures with a plasmonic effect provide colors with high resolution and high efficiency.[49,50] The assembly of colloidal crystals with structural colors also shows good properties with low-cost and large-scale fabrication by approaches such as coating,[51,52] microfluidics,[53,54] and ink-jet printings.[55,56] Furthermore, structural colors hold advantages not only in the method of color decoration but also can be endowed with functions such as solar energy conversion,[57,58] anti-counterfeiting,[59–61] and information encryption.[62–65]

In the present paper, we review the recent investigations on several major types of structural colors, including multilayer films, photonic crystals, and metallic metasurfaces. Moreover, the timeline of representative work reported in the past 20 years is given in Figure 1. We also discuss the approaches based on different physical principles to generate dynamically tunable structural colors. In addition, we summarize the reviewed works and prospects for the future.

Colors from Films

Multilayer Films. Structural colors based on film interference widely exist in nature, and thin-film interference structures, such as soap bubbles, and the beetle *Chrysina resplendens*, show golden color with more than 120 layers of film on the shell surface.[68] For the structure of multilayer, the interference can be understood as a pair of periodically superimposed thin layers.[69] Here, the transmission matrix theory is a method to calculate the transmissivity and reflectivity of multilayer films. For multilayers of non-magnetic materials, it can be calculated using the formula as follows:

$$\begin{bmatrix} B \\ C \end{bmatrix} = \left\{ \prod_{j=1}^{K} \begin{bmatrix} \cos\delta_j & \frac{i}{\eta_j}\sin\delta_j \\ i\eta_j \sin\delta_j & \cos\delta_j \end{bmatrix} \right\} \begin{bmatrix} 1 \\ \eta_{K+1} \end{bmatrix}$$

Multilayer films are depicted in Figure 2A, where K is the number of the layers, δ_j is the phase of the layer j, $\delta_j = \frac{2\pi}{\lambda} n_j d_j \cos\theta_j$, n_j is the refractive index of layer j, d_j is the thickness of layer j, λ is the wavelength of incident light

Review

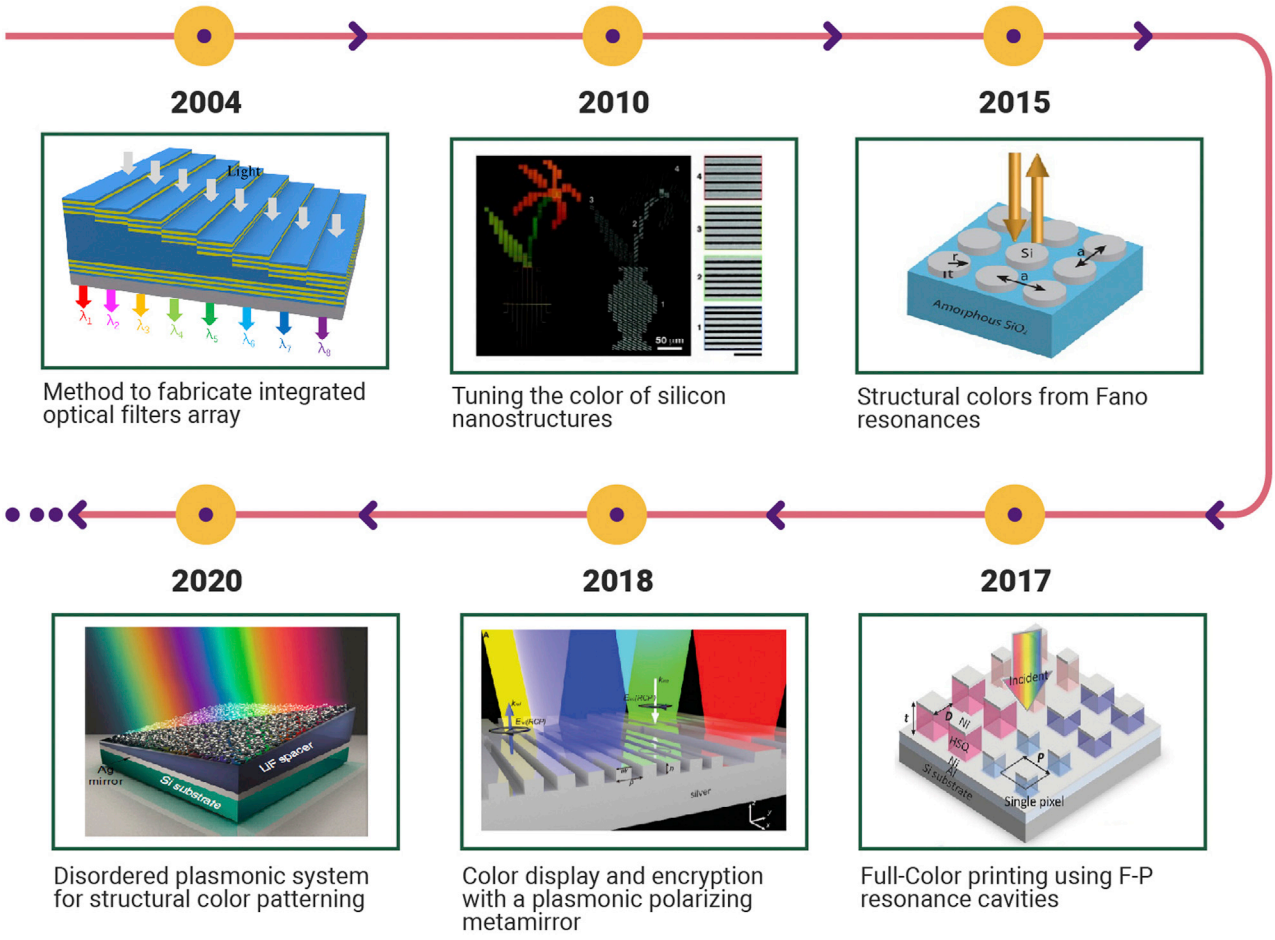

Figure 1. The Timeline of Structural Colors Reprinted by permission of American Chemical Society[44] (copyright, 2010, American Chemical Society), American Chemical Society[30] (copyright, 2015, American Chemical Society), Wiley Publishers[66] (copyright, 2017, Wiley Publishers), permission from Xiangang Luo et al.[63] (copyright, 2018, Springer Nature) and Peng Mao et al.[67] (copyright, 2020, Springer Nature).

under vacuum, θ_j is the angle between light in layer j and normal, and η_j is the admittance of layer j. For the *S*-polarization light, $\eta_j = n_j/cos\theta_j$. For the *P*-polarization light, $\eta_j = n_j cos\theta_j$.

Finally, the reflectivity and transmissivity of multilayer films can be calculated as follows:

$$R = \left(\frac{\eta_0 B - C}{\eta_0 B + C}\right)\left(\frac{\eta_0 B - C}{\eta_0 B + C}\right)^*$$

$$T = \frac{4\eta_0 \eta_{k+1}}{(\eta_0 B + C)(\eta_0 B + C)^*}$$

Structural colors based on multilayer films widely exist in daily life. The *Morpho* butterflies can show a stable bluish color from a wide range of viewing angles, which is unlike beetles or birds' feathers, which show different colors from different angles. Thin-film color reflectors inspired by *Morpho* butterflies were fabricated by Jung H. Shin and his coworkers[5] in 2012. The thin film is composed of a disordered silica microsphere layer, 300 nm of chromium (Cr), and eight pairs of TiO_2 and SiO_2 layers (Figure 3A). Their work has shown us a thin, flexible reflector that can be applied to the surface of a nonplanar object. It can be folded in half repeatedly while maintaining the bright color and angle-independent iridescence of the films. Moreover, large-scale colors ranging from *Morpho* blue to coppery red can be realized with larger deposition systems.

Conventional multilayer films have been widely used in daily life, such as in car window screens, camera lenses, and selective solar absorbers. However, investigation of functional devices with colorful film decoration is rare. Most of the solar absorber's color is monotonous black or dark blue. Due to the lack of color options, conventional solar selective absorbers are restricted from being applied in fields like architecture, where colorful surfaces are preferred. In 2015, Shaowei Wang and coworkers reported high-performance colored selective absorbers for architecturally integrated solar applications.[58] They realized the colorful solar absorbers based on multilayer films, which are more vivid compared with traditional ones, matching the requirement of architectural integration and leading to broader utilization of solar technologies. The color can be tuned over a wide range by changing the thickness of each layer while maintaining the high energy performance (Figure 3B). This type of absorber can be coated on various types of substrates. Patterned absorbers with different colors on a single substrate are demonstrated by them with 16 colored solar absorber units constructed of $Cu/TiN_xO_y/TiO_2/Si_3N_4/SiO_2$.[57] The combinatorial deposition process is used to integrate SiO_2 layers with different thicknesses on a single substrate (Figure 3C). The colored solar selective absorber array can have designable patterns and colorful appearance while maintaining high energy efficiency. It makes solar absorbers more flexible in fields like military camouflage and architecture integration. In 2019, Masateru M. Ito and coworkers developed the organized microfilbrillation (OM)technology.[70] This approach realizes structural colors by controlling the "craze," which is generated when the material is subjected to stress. This investigation of OM inkless color printing achieves high-resolution printing with 1.4×10^4 dots per inch (DPI). It can be further applied and expanded in many fields, such as banknote security, product packaging, and health care.

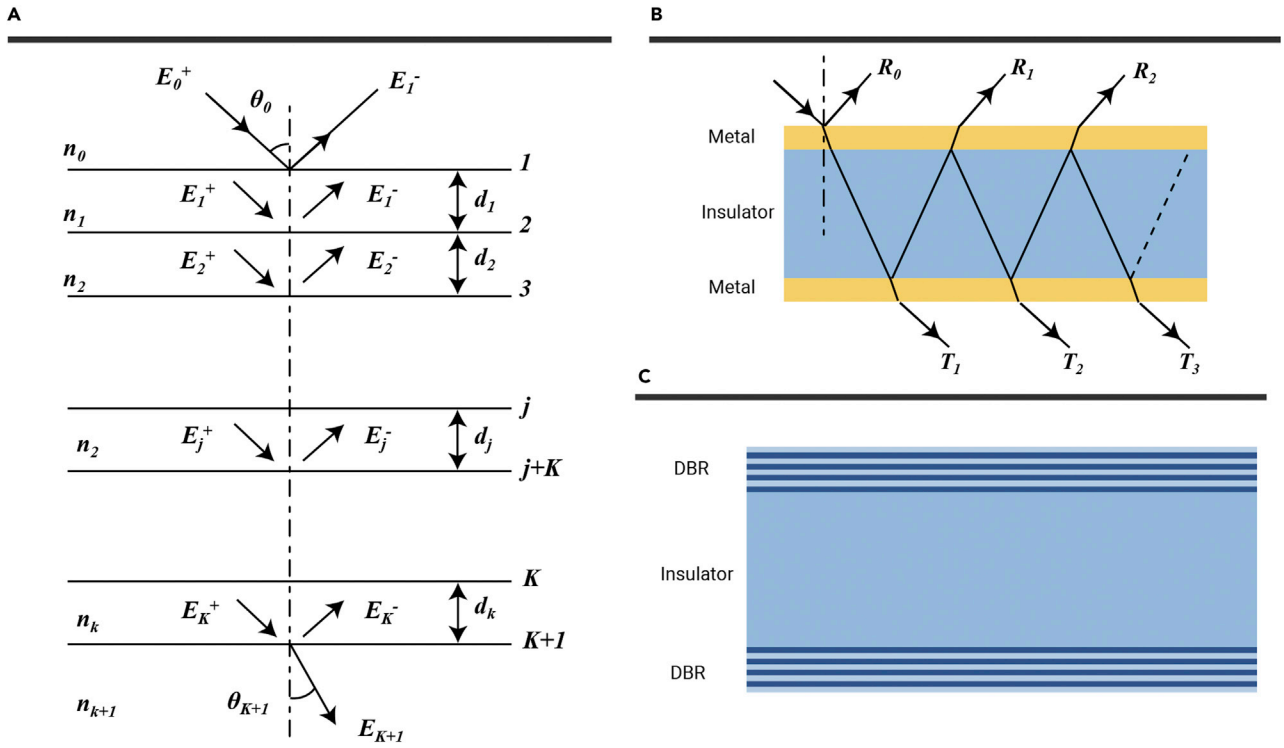

Figure 2. Interference of Light through Multilayer Films and F-P Cavity (A) The transmission matrix theory to calculate multilayer films. (B) MIM structure. (C) DBR-insulator-DBR structure.

The approaches and structures reviewed above show that structural colors based on multilayer films have been applied and remain promising on flexible substrates. Films are fabricated by deposition without a complex nanofabrication process. It is convenient to obtain colors by adjusting the thickness of each layer. Besides, multilayer films can be integrated on a single substrate to form a high-resolution image or decoration in the architecture field.

Fabry-Perot Cavity. Fabry-Perot (F-P) cavity resonances happen in a dielectric layer sandwiched by two reflectors, and the triple-layer structure of metal-insulator-metal (MIM) has been widely investigated for color filters (Figure 2A).[71–76] Constructive interferences take place when integer wavelength differences in the optical paths are reflected from the top and bottom surfaces, leading to different resonance wavelengths of the structural colors. Structural colors based on the traditional F-P cavity do not require time-consuming and high-cost nanofabrication techniques, such as e-beam lithography (EBL) or focused ion beam (FIB). Therefore, it is promising for various large-area applications, including photovoltaics,[77] and thermophotovoltaics.[57,58] In 2004, Shaowei Wang et al.[78] developed the concept of an integrated F-P cavity on a single substrate to manipulate the spectrum of light. In contrast with the conventional MIM F-P cavity, a distributed Bragg reflector (DBR) is used instead of the metal reflector (Figure 2B). Integrated narrow bandpass filters (NBPFs) with 16 × 1 linear array and 16 × 8 channels have been demonstrated by the combinatorial etching technique and combinatorial deposition technique, respectively.[79–82] The integrated optical filters are valid in both visible and infrared regions for high-resolution miniature spectrometers.[83,84] By decreasing the number of DBR layers, vivid colors can be achieved with simplified structure, which is able to be applied in display and inkless printing field.

Conventional F-P structure composed of two metallic mirrors separated by lossless dielectric material can achieve high absorption[85] or transmission.[86,87] The constructive interference of incoming and reflected waves forms the standing wave, and most optical power is absorbed by the top metallic reflector (Figure 4A[2]). In 2015, Aydin and coworkers demonstrated a transmission F-P color filter that is composed of a lossless dielectric material cavity and two silver (Ag) reflectors.[75] Figure 4A(1) depicts the schematic drawing of the F-P color filter with corresponding parameters. The F-P cavity can filter sunlight into individual colors covering the entire visible range by adjusting the thickness of the dielectric layer. Figure 4A illustrates the changes in transmittance spectrum as a function of SiO_2 thickness, and the color filter is angle dependent. The characteristics of angular dependence can support various applications, including directional thermal emitters and angle-sensitive absorbers. For display, imaging, and color printing applications, a high-angle tolerance color filter is desired, which is hard to realize with ordinary lossless F-P resonance cavities.[73,85] Much effort has been made to implement angularly robust F-P resonant structure filters. There are many approaches to improve the angle tolerance of the F-P cavity, such as the utilization of high refractive index materials, enhancement of interference effects in lossy nanocavities, phase compensation, and reduction of film thickness.[71,86,88–90]

The narrow absorption bandwidth leads to low brightness and purity, which can be solved by utilizing broadband absorption material on the top of the MIM structure. In contrast with Ag of low optical absorption loss in the visible range, nickel (Ni) is extremely lossy in the entire visible range, making it able to achieve broadband absorption. The schematic diagram of the proposed reflective color filter consists of an ultrathin (6 nm) Ni layer, an SiO_2 dielectric layer, and a thick Al layer (Figure 4B).[71] The measured reflectance spectra of differently fabricated F-P cavities vary with the thickness of SiO_2. The brightness of many proposed color filters is insufficient due to the narrow transmission or reflection band. Because of the broadband optical loss of Ni, this type of color filter shows abundant structural colors with high saturation and brightness over the entire visible range. Besides, this type of color filter has a certain degree of angle independence. The color of the fabricated filter does not change when the observation angle is below 60°, while it slightly changes when the observation angle becomes larger than 60°.

Due to the constructive interference mechanism, the spatial resolution of F-P resonance-based structural colors is inherently limited. The tri-layer F-P type reflective color filters have been investigated for high-resolution color

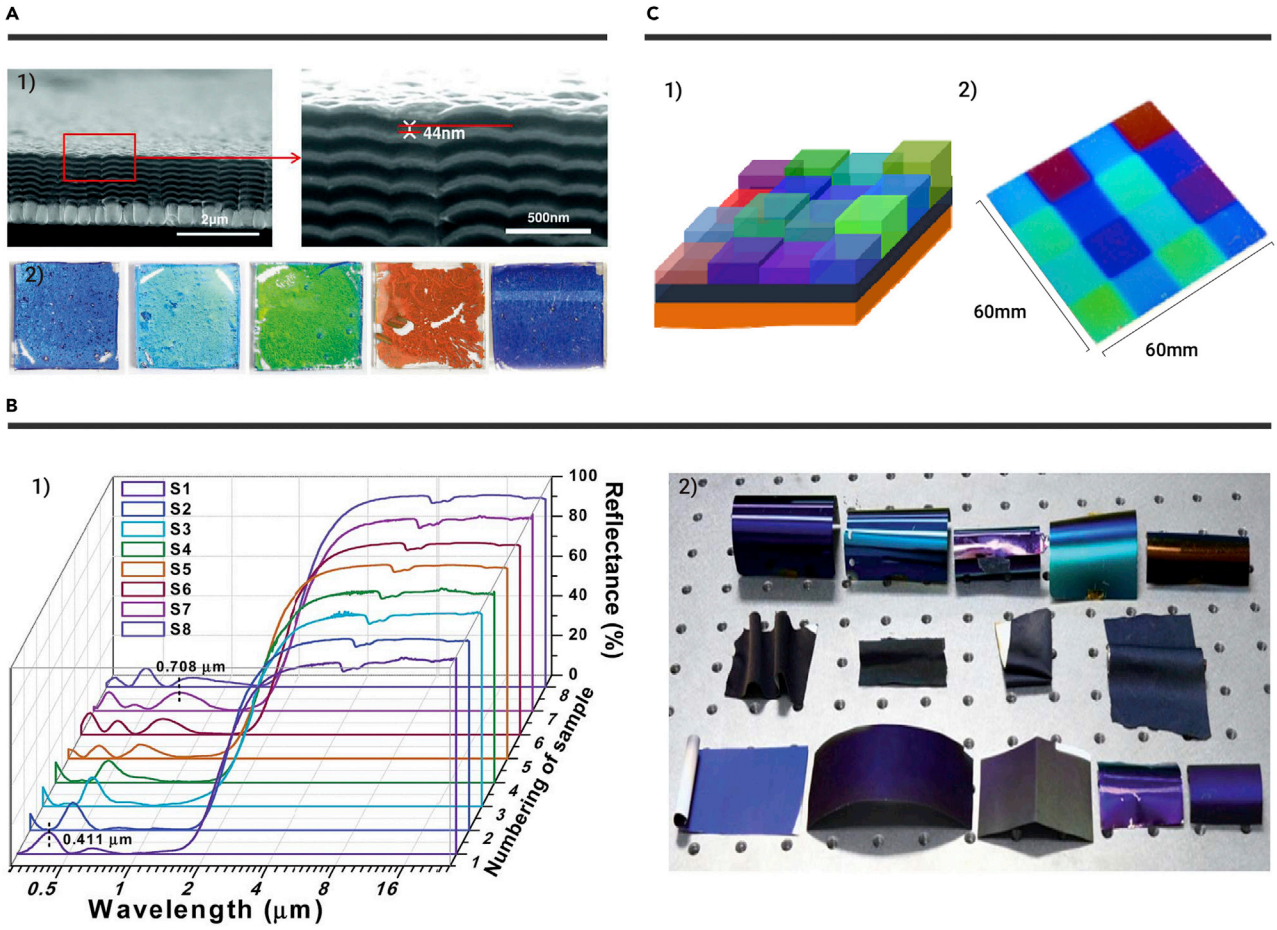

Figure 3. Colors from Multilayer Films (A) Structural color reflectors inspired by Morpho butterfly wings. (1) Cross-sectional SEM image of multilayer thin film. Scale bars: 2 μm and 500 nm. (2) Various colors ranging from deep blue through green to coppery red realized by controlling the layer thicknesses.[5] Reprinted by permission of Wiley Publishers (copyright, 2012, Wiley Publishers). (B) High-performance colored selective absorbers for architecturally integrated solar applications. (1) The measured reflectance spectra of the fabricated selective solar absorber samples. (2) Photograph showing the colored selective solar absorbers deposited on different types of flexible substrates.[58] Reprinted by permission of the Royal Society of Chemistry (copyright, 2015, Royal Society of Chemistry). (C) Colorful solar selective absorber integrated with different colored units. (1) Schematic diagram of monolithic integrated colored solar selective absorber array. (2) Photograph of the fabricated 4 × 4 colored solar selective absorber array.[57] Reprinted by permission of Optical Society of America (copyright, 2016, Optical Society of America).

printing.[71] By combining the conventional fabrication process with the grayscale lithography process, different colors can be obtained by adjusting the thickness of the dielectric layer. Huigao Duan's team has demonstrated a new printing concept by using the grayscale-patterned F-P resonance cavity.[66] Different from the traditional F-P type structural color,[71,85] their strategy shows that abundant colors can be obtained by varying the filling density of the F-P cavity. The schematic diagram shown in Figure 4C explains how to convert the obtained palette to reproduce van Gogh's Still Life: Vase with Twelve Sunflowers. This work provides the opportunity to use F-P cavities for high-resolution and full-color printing applications. In 2019, Yiting Yu and coworkers fabricated the asymmetric ultrathin F-P-type lossy cavity to realize vivid flexible structural colors, featuring wide gamut, angle insensitivity, high resolution, and good flexibility.[91] A wide color gamut is obtained by changing the thickness of the middle amorphous silicon (Si) and the top metal layer (Figure 4D[2]). The angle-independent tolerance of incident light is up to 60°, with a super-high spatial resolution (up to 10^5 DPI). The F-P resonance structure has the advantages of long-term stable and environmentally friendly properties over conventional dye pigments. The reflection or transmission spectrum can be easily tuned by changing the thickness of the insulator layer or metal layer. Benefiting from the highly precise micro-nano fabrication process, high-resolution color printing can be realized by conventional F-P cavity structures. The process of EBL and FIB can integrate a number of F-P cavities on the monolithic substrate, and form reflective RGB (red, green, and blue) or transmissive CMY (cyan, magenta, and yellow) pixels with high resolution. Furthermore, introducing an additional film layer[88,92] or reducing the thickness of the film structure can lighten the angle-dependent color effect, and the viewing angle can be improved to 60° as many investigations have reported.

Colors from Metasurfaces and Photonic Crystals

Newton first suggested that the color of birds and insects is perhaps produced by thin-film structures, so biologically inspired structural colors have been studied for centuries.[93] The wings of butterflies are a combination of optical gratings, multilayer films, and photonic crystals, giving rise to complex color mixing.[94] Photonic crystals and metasurfaces are crucial principles to form the creatures' colors in nature, which have also been extensively investigated to create artificial structural colors.[33,44,47,48,95–106] Here, we discuss recent progress on structural colors in metasurface structures and dielectric photonic crystal structures, including the assembly of colloidal microspheres.

Dielectric Metasurfaces and Photonic Crystals. Photonic crystal color filters have been proposed and experimentally fabricated for decades. As one of the most abundant elements on earth, the optical property of Si that generates colors has been widely investigated. The Si-based metasurface nanostructure can trap light and build up a high-intensity field when the wavelength of incident light matches the resonance mode, and the light is scattered to the far field as the leaky nature of nanostructures. In 2010, Linyou Cao et al.[44] studied the capability of Si nanostructures to generate visible colors based on Mie resonance, and demonstrated the structures of

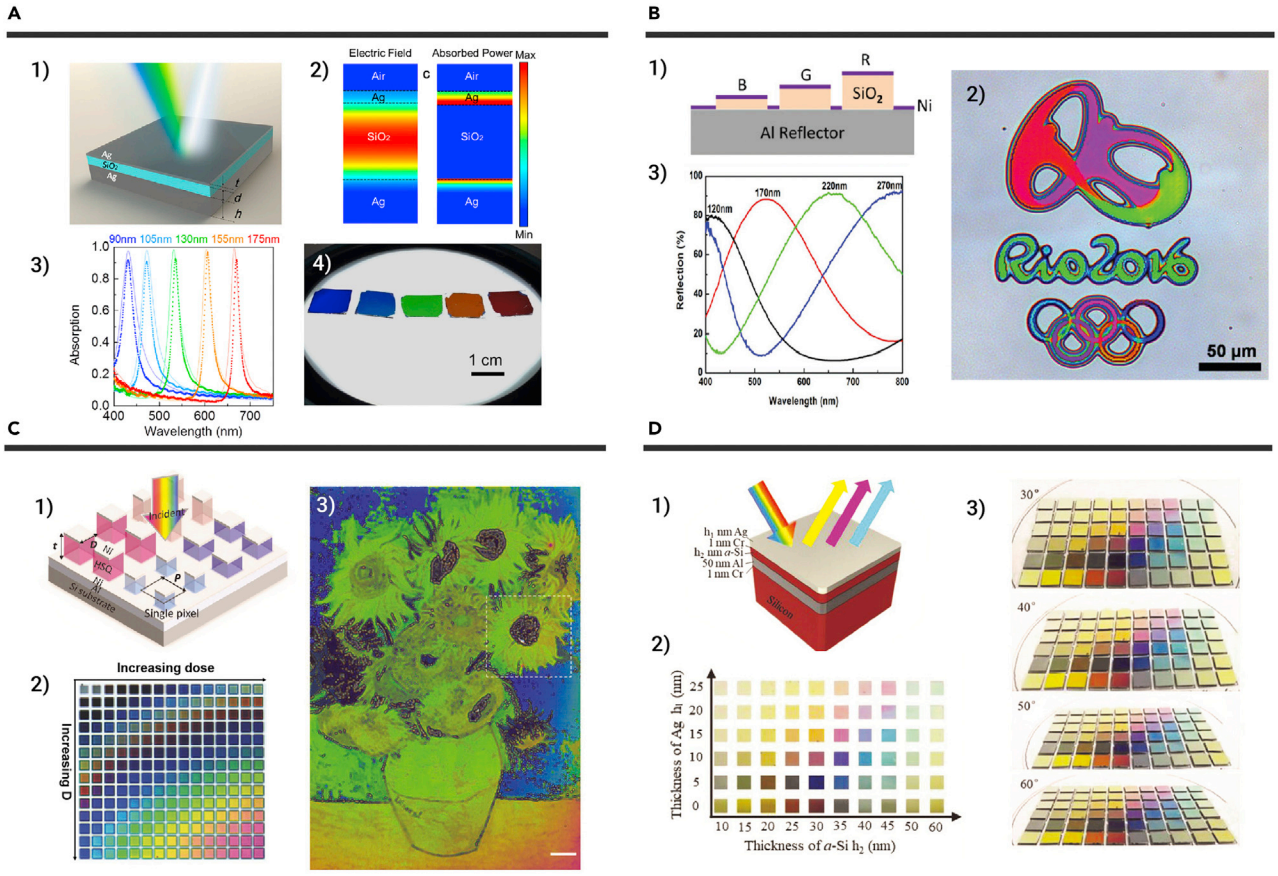

Figure 4. Colors from F-P Cavity (A) Large-area, lithography-free super absorbers, and color filters at visible frequencies using ultrathin metallic films. (1) Schematic configurations of the planar F-P cavity. (2) Electric field intensity profile and absorbed power distribution for the MIM filter. (3) The experimental (dots) and simulated (solid lines) transmittance spectra for F-P cavities. (4) Photograph of five different large-area color filters.[75] Reprinted by permission of American Chemical Society (copyright, 2017, American Chemical Society). (B) Reflective color filters and monolithic color printing based on asymmetric Fabry-Perot cavities using nickel as a broadband absorber. (1) Schematic drawing of a planar Ni/SiO_2/Al cavity. (2) The experimental reflection spectra for the F-P cavities. (3) The full-color micro logo of 2016 Rio de Janeiro Olympic Games.[71] Reprinted by permission of Wiley Publishers (copyright, 2016, Wiley Publishers). (C) Microscopic interference full-color printing using grayscale-patterned Fabry-Perot resonance cavities. (1) Schematic configuration of the grayscale-patterned F-P cavities. (2) The establishment of the database correlating the color. (3) An optical image of the full-color reproduction of van Gogh's Still Life: Vase with Twelve Sunflowers. Scale bars, 50 μm.[66] Reprinted by permission of Wiley Publishers (copyright, 2017, Wiley Publishers). (D) Defining deep-subwavelength-resolution, wide-color-gamut, and large-viewing-angle flexible subtractive colors with an ultrathin asymmetric F-P lossy cavity. (1) Illustration of the proposed asymmetric F-P type lossy cavity for the realization of subtractive structural colors. (2) A recorded color palette of the reflective subtractive colors as functions of the thicknesses of the top Ag layer and the lossy medium layer in the cavity. (3) Photographs of the practical color palette taken under the outdoor ambient light with different incident angles.[91] Reprinted by permission of Wiley Publishers (copyright, 2019, Wiley Publishers).

nanowires (NWs) and nanoparticles (NPs) . The leaky mode resonances of individual NWs can be harnessed, and the scattering efficiency is a function of incident wavelength and diameter. Therefore, by changing the diameter of the NW element, the spectrum covering the entire visible range can be obtained (Figure 5A). The Si structure is hard to work efficiently due to its inherent high absorption in the visible spectral range. In contrast, filters based on guide mode resonance (GMR) with other dielectric materials exhibit high efficiency and narrow bandwidth.[85,107] Based on their resonance characteristic, GMR structures with dielectric materials are used to produce narrowband resonances and have been applied in many applications, especially in the field of color filters.[16,108–112] In 2014, polarization-controlled tunable color filters were demonstrated by Mohammad Jalal Uddin et al.[109] By fabricating subwavelength gratings based on Si_3N_4 (Figure 5B[1]), a reflection filter with high efficiency exceeding 90% and narrow bandwidth under 12 nm was realized. The color filter with periods of 300 nm exhibits green and blue colors for TE and TM polarizations, respectively (Figure 5B[2]). This was the first reported polarization-tunable GMR color filter operating in reflection, enhancing the efficiency to a higher level compared with former polymer-based[113] and metallic nanostructure[13,114] color filters. Besides, the dielectric-based GMR structure can provide narrow bandwidth resonance with high efficiency while maintaining a high degree of optical tunability (wavelength, polarization, and intensity).

Sharp reflectance light can also be produced by the Fano resonance effect on photonic crystal slabs.[117] Structural colors based on this mechanism exhibit the property of weak angular dependence and are easy to fabricate. In 2015, Yichen Shen et al.[30] reported structural colors produced by the Fano resonance effect on the thin photonic crystal slab (Figure 5C[1]). The incident light is confined on the surface as a one-dimensionally confined mode, which can interfere with the reflected light and produce sharp reflectance light (Figure 5C[2]). The interference lithography (IL) process is used to fabricate this structure.[75,118] Since the photonic crystal resonance directly controls the reflection spectrum, this structural color is angle independent. This work provides a versatile way to generate colors from dielectric metasurfaces, which can be applied in high-end displays, light-emitting devices, and many other fields.

In 2017, Xiaolong Zhu et al.[115] reported an approach to realize ink-free structural colors by resonant laser printing (RLP) on high-index dielectric metasurfaces. This investigation demonstrated laser-printable structural colors with all-dielectric materials. As shown in the schematic diagram in Figure 5D,[115] the metasurfaces are fabricated by nanoimprinted polymer pillars, with a thin film of Ge deposited. Thereafter, the Ge metasurfaces are treated by laser to tune the morphology-dependent optical resonance. The energy of the pulsed laser leads to the morphological change of Ge metasurfaces and can obtain colors covering all the visible wavelengths. Figure 5D(3–4) shows

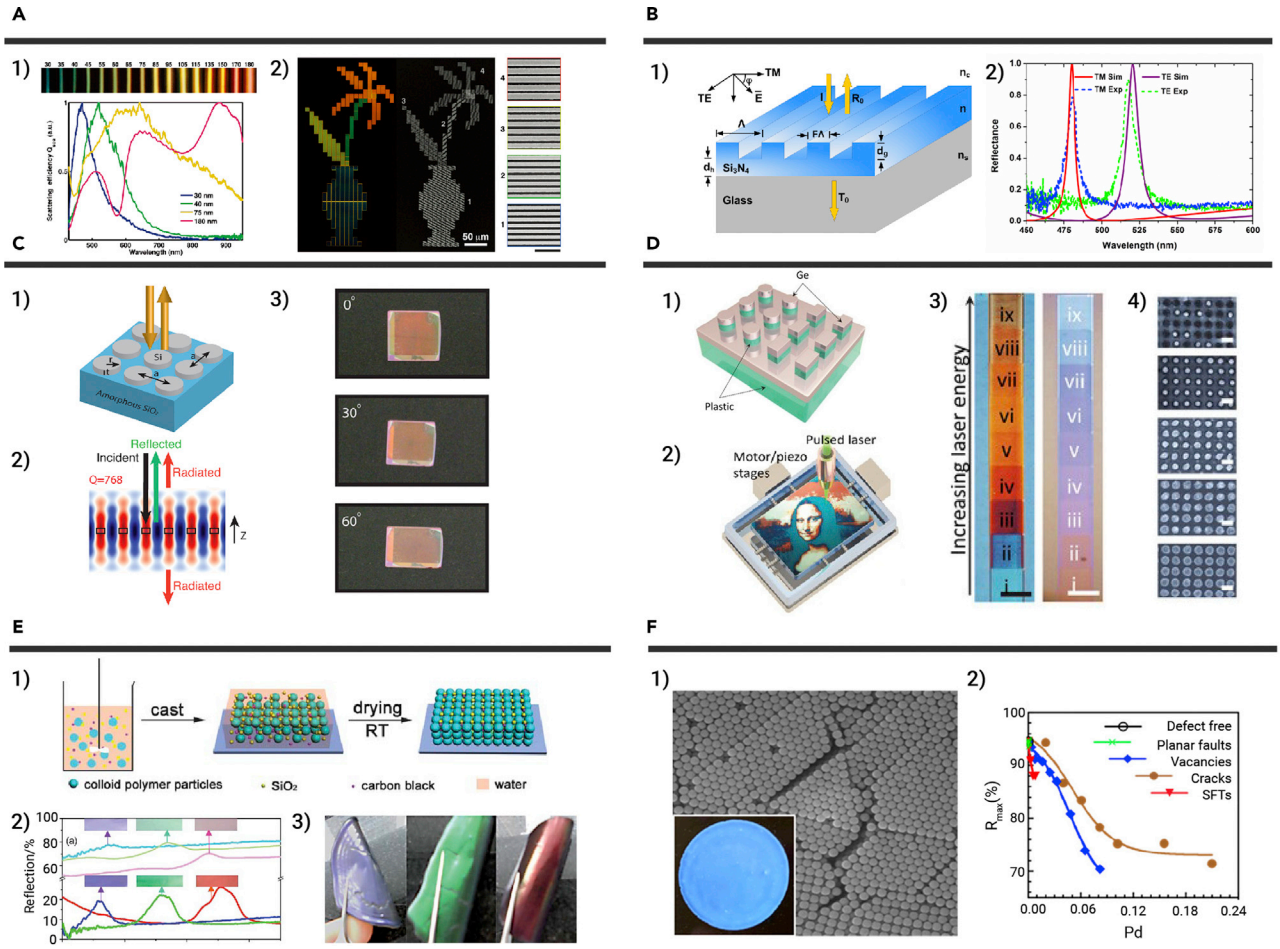

Figure 5. Colors from Dielectric Metasurfaces and Photonic Crystals (A) Tuning the color of silicon nanostructures. (1) Darkfield optical images and spectral scattering efficiency are taken from selected Si NWs of different diameters. (2) Darkfield optical images and SEM images of large-scale patterned NW arrays.[44] Reprinted by permission of American Chemical Society (copyright, 2010, American Chemical Society). (B) Guided-mode resonant polarization-controlled tunable color filters. (1) Dielectric GMR color filter structure. (2) The experimental and theoretical reflectance of the blue-green tunable filter.[109] Reprinted by permission of Optical Society of America (copyright, 2014, Optical Society of America). (C) Structural colors from Fano resonances. (1) Illustration of the simulated structure. (2) A vertical slice of the spatial distribution of the electric field for the resonant mode responsible for the reflectance peak. (3) Photographs of the fabricated sample with different viewing angles.[30] Reprinted by permission of American Chemical Society (copyright, 2015, American Chemical Society). (D) RLP of structural colors on high-index dielectric metasurfaces. (1) Schematic diagram of the structures. (2) Schematic setup of RLP. (3) Reflection and transmission microimages of multicolored structures generated by gradually increasing laser powers. (4) Corresponding SEM images of the microstructures (i, iii, v, vii, and ix) in (3).[115] Scale bar in (3) and (4) represents 0.5mm and 200nm. Reprinted by permission of the American Association for the Advancement of Science (copyright, 2017, American Association for the Advancement of Science). (E) Large-scale fabrication of three-dimensionally ordered polymer films with strong structure colors and robust mechanical properties. (1) Illustration of the fabrication procedure of the polymer ordered films. (2) Experimental reflection spectra of crystal films with different polymer sphere diameters. (3) Bent polymer/silica/carbon black crystal films.[102] Reprinted by permission of the Royal Society of Chemistry (copyright, 2012, The Royal Society of Chemistry). (F) Effect of defective microstructure and film thickness on the reflective structural color of self-assembled colloidal crystals. (1) Typical SEM image of the top surface of a colloidal crystal film. (2) Compilation of peak reflectance Rmax as a function of defect density ρd added to the system for the set of defect types studied.[116] Reprinted by permission of American Chemical Society (copyright, 2020, American Chemical Society).

the color change under different laser energies and corresponding SEM images of the structure. Since the scale of resonators is subwavelength, the localized resonances make the reflected colors angle independent with incident angles up to 60°. It is a new way to print stable, large-scale, angle-independent, and vibrant structural colors. Due to the sub-diffraction spatial field modulation, the resolution of printing colors can exceed 10^5 DPI. This structural color is flexible to design the image or pattern, which has a wide scope of application fields, such as encrypting, data storage, and retina devices.

For the above-mentioned conventional photonic crystal structural colors, a precise and expensive fabrication process is necessary, which restricts the large-scale and low-cost fabrication. In contrast, the self-assembly of colloidal crystal has the advantage of its simple and low-cost fabrication process with good structural color properties. Moreover, the optical properties of assembled colloidal microspheres have been investigated for decades.[119–122] In 2012, Limin Wu and coworkers proposed the three-dimensionally ordered polymer films with strong structural colors and robust mechanical properties.[102] Figure 5E shows the simple fabrication process of the crystal film. Without any special equipment or complex process, the polymer crystal films are easily obtained by directly casting the suspension on substrates. The reflection spectra are mainly affected by the diameter of polymer spheres, and the content of carbon black can modulate the chroma of structural colors. Figure 5E(2–3) depicts the reflection spectra of the polymer crystal films with varying diameters, which exhibit blue, green, and red structural colors, with and without carbon black. This work provides a way to obtain large-scalable structural colors with controllable and robust mechanical properties. For most investigations, the effect of defective microstructure on structural colors is seldom investigated systematically. During the solvent evaporation process, the defect of the assembled photonic crystal will be created, affecting the spectra of reflective structural colors (Figure 5F). In 2020, Michael J. Solomon and coworkers reported their work on the effects of defective microstructure and film thickness on the reflective structural color of self-assembled colloidal crystals.[116] Figure 5F(2) shows the effect of

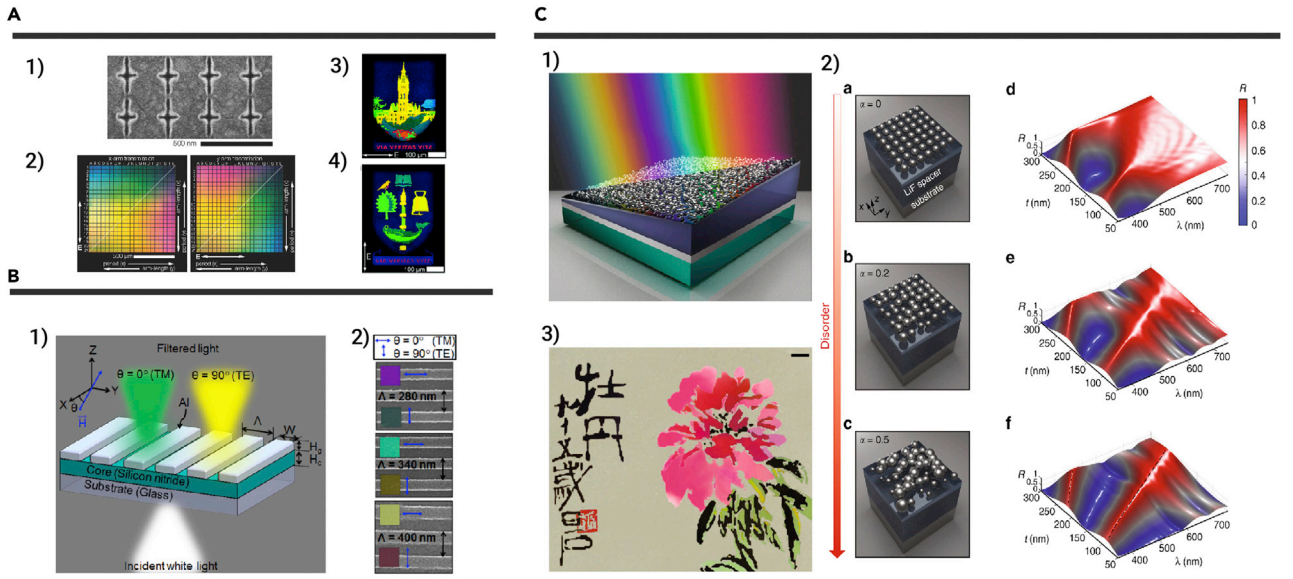

Figure 6. Colors from Metal Metasurfaces (A) Plasmonic color filters as dual-state nanopixels for high-density microimage encoding. (1) The SEM images of nano cross-shaped aperture arrays on an Al film. (2) Bright-field microscope images showing a switchable color palette. (3 and 4) Bright-field transmission images showing the full-color pictures.[129] Reprinted by permission of Wiley Publishers (copyright, 2017, Wiley Publishers). (B) Polarization-controlled broad color palette based on an ultrathin one-dimensional resonant grating structure. (1) Schematic diagram of the metal-based color filter where the white incident light is filtered into different colors depending on the polarization. (2) SEM images of proposed devices with different periods.[137] Reprinted with permission from Ishwor Koirala et al.[137] (copyright, 2017, Springer Nature). (C) Manipulating disordered plasmonic systems by an external cavity with the transition from broadband absorption to reconfigurable reflection. (1) Schematic diagram of the sample with Ag nanoclusters on a spacer with gradually varying thickness. (2) Schematic diagram of platforms with differently disordered parameters and the corresponding reflection spectra as a function of spacer thickness. (3) The fabricated hybrid structure.[67] Reprinted with permission from Peng Mao et al.[67] (copyright, 2020, Springer Nature).

commonly observed defect types (vacancies, stacking fault tetrahedra, planar faults, and microcracks) on the peak intensity of structural colors. The results show that the scales of peak intensity are reduced with increased defect density, and it is less sensitive to the type of defect compared with its volume. The physical principle of structural colors generated by crystalline structures can be more clearly identified.

In summary, as the dielectric materials are transparent and lossless in the visible spectral range, structural colors generated from the dielectric metasurfaces and photonic crystals hold high efficiency and narrow spectral bands. The Mie resonance and Fano resonance can create sharp reflection spectra over a wide range of viewing angles. GMR mode working with dielectric grating shows different images under TM- and TE-polarized light. Besides, the morphology can be manipulated by different laser energies. Compared with the F-P cavity and multilayer principle, dielectric metasurfaces can generate colors with angle independence and higher resolution, which can be used in high-resolution displays, holographic technologies, and so on. Meanwhile, the self-assembly of colloidal photonic crystals is a low-cost and large-scale approach to generate angle-independent, robust, and flexible structural colors. However, high resolution of self-assembled colloidal photonic crystal colors is hard to achieve, being restricted by the fabrication process. However, it is still promising for applications of anti-counterfeiting, intelligent sensors, and so on.

Metal Metasurfaces. With the development of the nanofabrication process, the morphological characteristics of metallic nanostructures can be well controlled with high precision.[123] The resolution of metallic structural colors can be improved beyond the optical diffraction limit.[41] Compared with dielectric metasurfaces, the metallic structure is chemically stable with fewer fabrication processes while maintaining geometry-dependent spectral resonance. Surface plasmon at the metal-dielectric interface offers opportunities to broaden the definition of structural colors.[124] Due to the capability of strong field localization, the plasmonic nanostructures are promising in structural color applications.[125–128] The surface plasmon resonance (SPR) can be tuned by the incident angle and polarization, making the dense optical data archival[129] and other security applications possible. Metal nanostructures in various morphologies, such as nanohole arrays,[130,131] and nanopixels based on metallic films,[129,132] have been widely investigated. The principles of metallic nanoantenna,[41,50,133,134] metallic GMR grating,[135] and disordered plasmonic systems[67] are widely investigated.

H. F. Ghaemi et al.[136] demonstrated the extraordinary optical transmissions through periodic subwavelength hole arrays in optically thick metallic films. In 2007, the optical properties of tiny subwavelength holes in the metal film were reviewed by C. Genet and T. W. Ebbesen.[131] The array of dimples on Ag film can be prepared by FIB. Although the periodicities of metallic nanohole arrays are all larger than half of the corresponding wavelength, their resolution is quite high compared with chemical pigments. Therefore, it can satisfy many requirements for practical applications compared with conventional pigments. Except for nanoholes, by using the nanofabrication process, metal-based nanostructures can be designed to store more than one image in one pixel by utilizing the polarization property of asymmetrical structures. In 2014, Xiao Ming Goh et al.[133] demonstrated a three-dimensional plasmonic stereoscopic printing technique. The polarization-sensitive color pixels are achieved with aluminum (Al)-coupled nano square pair and elliptical nanodisks with complementary holes at the bottom Al layer, which can display different images with differently polarized incident light. Therefore, two overlaid full-color images can be independently encoded into the same area. In 2017, Alasdair W. Clark and coworkers presented an approach to encode two datasets into one set of pixels for the first time.[129] By using the asymmetric cross-shaped plasmonic nanoapertures on Al thin film (Figure 6A), each aperture is designed with two independent resonances. Therefore, double the amount of information can be stored in one unit pixel. This structure inherently has polarization ability due to its cross-shaped nanoslit. The resonance of two orthogonal arms can be independently tuned. Colors ranging across the full visible spectrum at each polarization of white light can be produced by encoding the arm length and the period of arrays (Figure 6A[2]). As shown in Figure 6A(3–4), the surface plasmon-based pixels are capable of producing dual, polarization-switchable information states into the same area, and the resolution can achieve 10^5 PPI at most. This dual-state microimage encoding approach provides a useful way to enhance the information density. It is promising for applications in fields such as counterfeit-prevention measures and high-resolution printing.

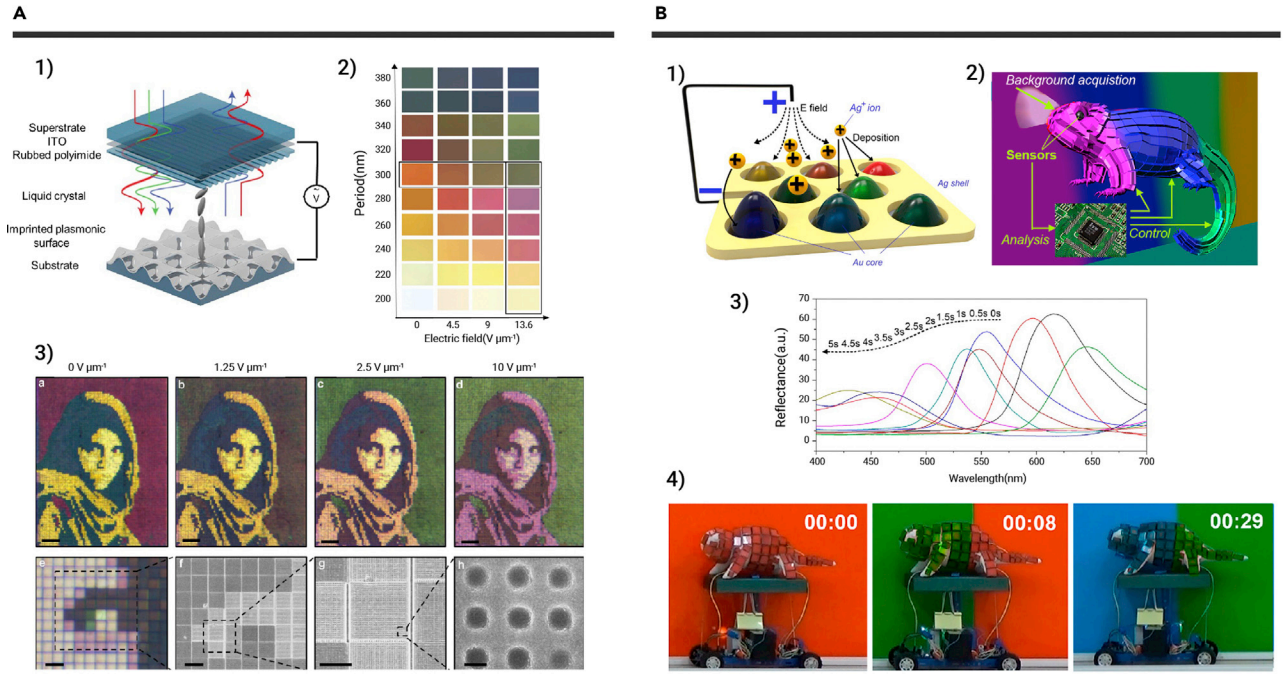

Figure 7. Dynamically Tunable Structural Colors Generated by Plasmonic (A) Polarization-independent actively tunable color generation on imprinted plasmonic surfaces. (1) Schematic diagram of the plasmonic-liquid crystal cell. (2) The palette of obtainable color. Microscope images of a singular Afghan Girl image as a function of the applied electric field, and (3) SEM images of the sample before fabrication into a liquid crystal cell.[154] Reprinted by permission of Springer Nature (copyright, 2015, Springer Nature). (B) Mechanical chameleon through dynamic real-time plasmonic tuning. (1) Schematic diagram of the plasmonic cell. (2) Schematic diagram of the plastic chameleon covered with armor-like plasmonic cells. (3) Reflection spectra of the device after different electrodeposition times. (4) Screenshot of the plasmonic chameleon demonstration movie.[159] Reprinted by permission of American Chemical Society (copyright, 2016, American Chemical Society).

Over the past decades, various plasmonic color nanotechnology-based localized surface plasmon resonances (LSPRs), such as nanopost arrays,[41] hybridized antenna-hole arrays,[132] and all-metal nanostructures,[16,135] have been demonstrated. LSPR is related to standing surface plasmon waves, in which free-electron oscillations inside a metallic nanostructure are coupled to electromagnetic fields in a neighboring dielectric.[138] Different from SPR-based structural colors, which are conventionally sensitive with the incident angle and not desirable for some particular applications,[139] the LSPR-based structural colors are equipped to diminish the angle-sensitive characteristics due to the tight spatial localization of the electromagnetic field. Resonant plasmonic antennas efficiently localize the electromagnetic field, resulting in angle-insensitive vivid colors, which can be adjusted by the alteration of geometric dimension. Due to the tight spatial localization of light, structural colors based on LSPRs can allow printing with a resolution that beats the diffraction limit. In 2012, color printing nanotechnology with resolution approaching the optical diffraction limit was proposed by Joel K. W. Yang and coworkers.[41] By depositing the metal disk above hydrogen silsesquioxane (HSQ) pillars on a back reflector, the interaction between the back mirror and the resonances of disks can be manipulated by tuning the radius of the metal top disks and the separation between the pillars to affect the reflected color. The resulting print of the Lena image can have a resolution up to 10^5 DPI.

The metallic GMR structural colors have also been widely investigated in recent years. In contrast with dielectric GMR, the metallic GMR structure has a broader resonance bandwidth due to the loss of metal, which is more suitable for optical applications.[16,140,141] The polarization-controlled structural color based on metallic GMR has been reported by Ishwor Koirala et al.[137] The polarization-tuned metallic structural color is based on a one-dimensional resonant Al grating integrated with a Si_3N_4 waveguide deposited on the glass substrate (Figure 6B). Figure 6B(2) shows the SEM images of fabricated filters and the insert observed colors for TE and TM polarizations. The whole visible color is obtained by tailoring the polarization and metallic grating duty ratio. The results imply that iridescent vivid colors can be obtained with the aid of light polarization, which is a crucial property for applications, such as optical data storage. It is worth noting that, due to the physical mechanism of GMR, it should have tens of periods to approach adequate performance that limits the spatial resolution of the GMR structures.[142] Additionally, the optical response of the GMR structure is highly sensitive to the incident angles. There are many approaches to mitigate the angle-sensitive effect, such as by integrating the GMR structure with a gradient-index layer,[143] coating with a metal film,[144] real-time compensation via voltage-driven dispersed layer,[145] or assistance by integrated cavity resonator,[146] and so on.[135,147,148] Except for the morphology and parameters of the structure that can tune the colors, the disordered nanostructure system also shows good capability on structural colors. In 2020, Shuang Zhang and coworkers reported the manipulation of disordered plasmonic systems (Figure 6C).[67] By utilizing an external cavity under the disordered plasmonic system to manipulate the decay rate of a specific mode, the transition is realized from broadband absorption to tunable reflection (Figure 6C[2]). The Chinese watercolor printing The Peony Flower by Baishi Qi is printed by tuning the spacer thickness, and colors, including black, are formed well, which is hard to generate by conventional periodic structures (Figure 6C[3]). The random plasmonic system is material independent without a time-consuming lithography process. This approach provides a novel platform for various practical applications. Structural color imaging by plasmonic metasurface mosaic filters has also been investigated. For instance, Won-Jae Joo, Mark L. Brongersma, and coworkers introduced metasurface mirrors into organic light-emitting diodes (OLEDs), which can offer high luminescence efficiency and enhance the color purity of OLEDs, along with display resolution beyond 10^4 PPI.[134] Moreover, Yash D. Shah et al.[149] proposed an approach to realize ultralow-light-level color images by integrating the plasmonic metasurface and single-photon avalanche diode (SPAD) arrays.

Overall, high-quality metallic metasurface structural colors based on SPR and LSPR have been extensively investigated. Metallic GMR and disordered systems also exhibit great practical potential in many fields. The all-metal structures decrease the fabrication time and lower the cost while holding good color properties. For practical applications, the metallic metasurface colors are preferable in the aspects of high resolution and excellent durability

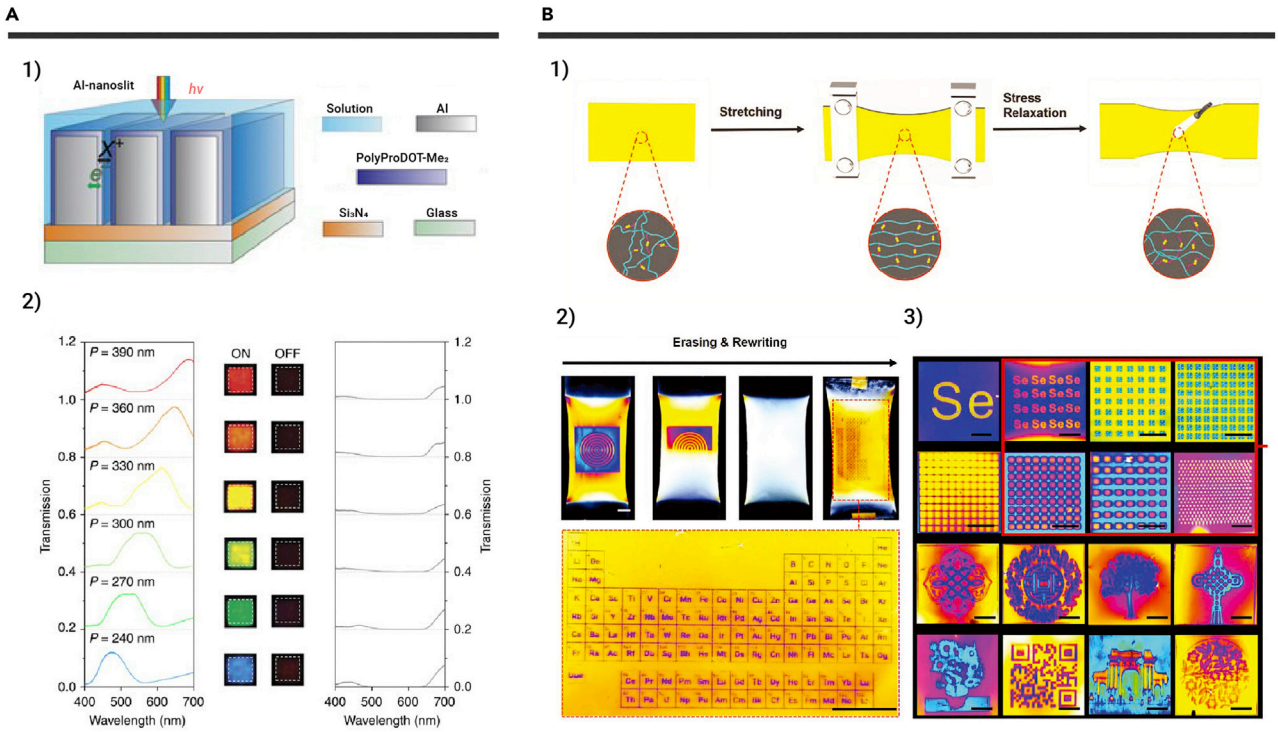

Figure 8. Dynamically Tunable Structural Colors Generated by Electrochromic Switching, and Diselenide Metathesis (A) High-contrast and fast electrochromic switching enabled by plasmonics. (1) Schematic diagram of a plasmonic electrochromic electrode incorporating an Al-nanoslit array. (2) On and off states of the polymer are displayed with their spectra, respectively.[164] Reprinted by permission of Springer Nature (copyright, 2015, Springer Nature). (B) Tunable structural color patterns based on the visible-light-responsive dynamic diselenide metathesis. (1) Scheme for the formation and regulation of stress in the material. (2) Erasing and rewriting processes of structural color pattern. The scale bar represents 4.5 mm. (3) Various patterns with different structural colors. The scale bar represents 2.5 mm.[165] Reprinted by permission of Wiley Publishers (copyright, 2020, Wiley Publishers).

due to the high precision of the micro-nano fabrication process and stability of metallic material. However, compared with dielectric metasurfaces, the intrinsic ohmic loss leads to low efficiency and broadband reflection spectral peak. There is still a long way to go to apply metallic metasurface structural colors in daily life.

Dynamically Tunable Structural Colors

Conventionally, most structures based on films, photonic crystals, and metasurfaces usually retain static and unchangeable color after fabrication, limiting their potential applications. Therefore, many approaches have been investigated to realize the dynamically tunable capacity of structural colors after fabrication. Here, we reviewed several main approaches to achieve tunable structural colors, including the approach of reconfigurable liquid crystals (LCs), electrochromic and plasmonic modulation, mechanical stretching, and self-assembled colloidal microspheres.

LCs are a widely used approach to achieve tunable structural colors. They are usually used to combine with structures, such as plasmonic metasurfaces.[150–155] Figure 7A illustrates the typical LC-based structural colors, which were reported by D. Franklin et al.[154] in 2015. The polarization-independent dynamically tunable color is generated on the imprinted plasmonic surfaces.[154] The LCs have the properties of reconfigurability and anisotropy. They are utilized to adjust the dielectric constant surrounding the metallic nanostructure, and affect the spectral location of plasmon resonance.[156–158] In this work, a birefringent LC and a periodic array of shallow nanowell are used. By varying the period of plasmonic nanowell arrays, color ranging across the entire visible spectrum was achieved for the first time. The reflection spectra of this LC cell are dynamically tunable with the applied voltage and nanostructure period (Figure 7A[2]). The images of Afghan Girl were fabricated, as shown in Figure 7A(3), along with the microscope and SEM images. Although the full range of color is obtained by this structure, the period is unchangeable once the nanowell is fabricated, and the spectrum can only be tuned in a limited range, making it hard to apply in fields requiring real-time and full visible range tunability. Subsequently, the RGB color based on a polarization-dependent LC-plasmonic system is demonstrated, with spectrum changing with applied voltage.[155]

Different from the approach of LC-plasmonic modulation, Guoping Wang et al.[159] demonstrated the real-time plasmonic tuning approach, which can modulate plasmonics through the combination of electrochemical bias and bimetallic nanodot arrays. Figure 7B shows that the Au core and Ag shell structures are fabricated by depositing and stripping processes. Reflection spectra of the device can be tuned over the entire visible range by changing the electrodeposition times and electrostripping times. By integrating the ordered nanodomes, a mechanical chameleon is fabricated to demonstrate this approach. The artificial mechanical chameleon can change its color according to the background color, as shown in Figure 7B(4). It can realize active camouflage under complex environments with the aid of color sensors and micro-control systems.

As the essential application of structural colors, the flat-panel display technology has great developmental potential. Researchers have found that the electrochromic materials have brilliant properties, such as vibrant colors, low cost, and relatively simple processing requirements, making them particularly advantageous in flexible display applications.[160–163] By utilizing the electrochromic materials in combination with plasmonic nanoslit arrays, Ting Xu et al.[164] demonstrated high-contrast full-color and fast electrochromic switching in 2016. Figure 8A shows a thin layer of polyaniline (PANI) (or polyproDOT-Me_2) coated on the Al (or Au) nanoslit arrays and immersed in the electrolyte solution. The electrons and ions flow in and out of the polymer when the voltage is applied to the electrode. The polymer's optical absorption characteristics change with its charge state. The full-color electrochromic optical response can be realized by tuning the period of nanoslits. Figure 8A(2) shows the color obtained by tuning the period ranging from 240 to 390 nm. By switching the applied voltage, the color can be tuned

Review

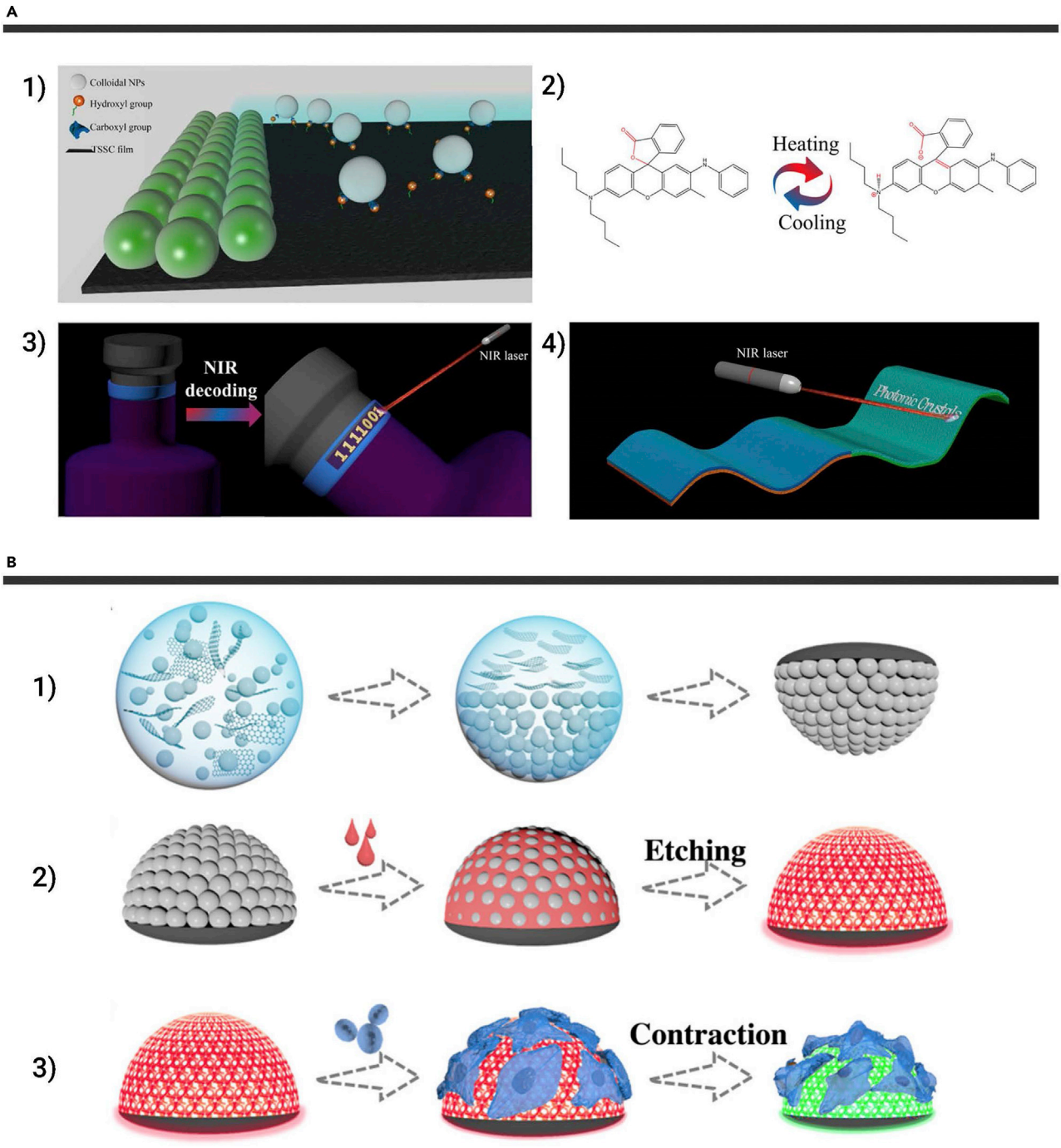

Figure 9. Dynamically Tunable Structural Colors Generated by Electrochromic Switching, and Diselenide Metathesis (A) Controllable structural colored screen for real-time display via NIR light. (1) Hydrogen bonding effect to increase the binding properties of TSSC films. (2) Thermosensitive molecular structures change after heating. (3) Schematic diagram of the information decoding process of TSSC labels. (4) Schematic diagram of the information recording process of multicolored TSSC films induced by the NIR laser.[105] Reprinted by permission of American Chemical Society (copyright, 2020, American Chemical Society). (B) Anisotropic SCPs from colloidal phase separation. (1) The generation process of the anisotropic Janus SCPs. (2) The preparation process of the anisotropic hydrogel SCPs. (3) Construction of cardiomyocyte monitoring platform by the anisotropic hydrogel SCPs.[100] Reprinted with permission from Yuanjin Zhao et al. (copyright, 2020, The Authors, American Association for the Advancement of Science).

between two states (on and off status corresponding to reduction and oxidation of polymer, respectively) with high speed and high contrast, which holds promise for applications ranging from catalysis to photovoltaics.

Flexible materials, such as polydimethylsiloxane (PDMS), usually can be used as a substrate to fabricate nanostructure,[166,167] and the structure period can be dynamically tuned by stretching the elastic substrate. In 2017, Ming Lun Tseng et al.[167] realized the dynamically tunable Al plasmonic arrays for the full-spectrum response by stretching the elastomeric substrate. The scattering color is sensitive to the lattice spacing. The spectrum of the plasmonic device can be tuned less than 35% of the maximum strain. The metasurface structure on the elastic substrate is not the only way to achieve tunable color. By employing the dynamic covalent bond (DCB), the structural color material is responsive to visible light. The diselenide metathesis is applied to release the fixed stress of stretched materials under visible light irradiation.[165] Figure 8B shows that the shape and stress are fixed during the shape-memory process. The stress can be further regulated with visible

Table 1. Categories of Structural Colors Classified by Principle

Type of Structural Color	Principle of Color Generation	Properties	Shortcomings
Multilayer films	• interference	• large-area fabrication • simple fabrication process	• sensitive to viewing angle • limited resolution
F-P cavity	• cavity resonance	• high saturation and brightness • polarization independent	• difficult to achieve high resolution at low cost
Dielectric metasurfaces and photonic crystals	• Mie scattering • Fano resonance	• high saturation and efficiency • insensitive to viewing angle	• difficult achieve to low-cost, large-scale production
Metallic metasurfaces	• surface plasma resonance • localized surface plasma resonance	• polarization dependence • high resolution • insensitive to viewing angle	• low efficiency due to the inherent loss of metal materials
GMR structure	• guide mode resonance	• high efficiency • favorable color purity	• limited resolution • sensitive to viewing angle

light irradiation. The photomasks are used to realize various patterns, and the patterning resolution reaches 6.2 μm. It can be erased by irradiation or releasing the stress completely and rewritten by another uniaxial stretching. The color is only visible when two polarizers are crossed, making it useful in the anti-counterfeiting field. Besides, the simple fabrication process makes it possible to realize large-scale preparation.

Compared with the above-mentioned approaches, the self-assembly of colloidal photonic crystals provides a simpler approach to tune the structural colors in real time. The dynamic tunability of assembled colloidal microspheres can be achieved by combining with tunable material, such as thermosensitive films,[105] reduced graphene oxide, and specific hydrogel.[100] Recently, Jie Wei and coworkers reported the strategy of controllable structural colored screens via near-infrared (NIR) light, which is based on the structure of colloidal NPs combined with thermosensitive film (Figure 9A).[105] The thermosensitive molecular structures have a precise temperature transition at 45°C. By using thermosensitive structural colored (TSSC) films, the NIR response anti-counterfeiting label and NIR direct writing colloidal crystal screen are demonstrated, which can transform the state from reflection to transmission under the exposure of the NIR laser in real time. The fabricated TSSC films exhibit properties of angle independence, excellent flexibility, and durability. These multicolored TSSC screens have great practical application potentials in information storage, anti-counterfeiting, and so on.

Due to the flexibility of the assembly process, the graphene oxide (GO) can also be co-assembled with colloid NPs by the microfluidic process. A few months ago, the anisotropic structural color particles (SCPs) with intelligent responsive capacity were proposed by Yuanjin Zhao et al.[100] Figure 9B shows that the SCPs are formatted by phase separation of GO and Si NPs in droplets. These anisotropic SCPs and their inverse opal hydrogel derivatives show brilliant structural colors and controllable capabilities. By choosing N-isopropylacrylamide (NIPAM) as monomer and N,N′-methylenebis (acrylamide) (Bis) as cross-linker, the thermal responsive particles are prepared (Figure 9B[2]). When the NIR light irradiates the particles, the pNIPAM can reversibly shrink and swell due to the photothermal effect of reduced GO, and the color changes at the same time. Furthermore, by using hydrogel methacrylated gelatin (GelMA), it can be used as microcarriers for the culture and monitoring of the cardiomyocytes (Figure 9B[3]). Besides, the structural color patch with anisotropic surface adhesion is inspired by the mechanisms of mussel adhesion and eyeball lubrication.[101] With the capability of real-time color response to mechanical strain, it can be used to monitor heartbeat activity. These types of SCPs in combination with GO have great potential in biomedical areas.

In summary, the dynamic tunability of structural colors can be achieved via many approaches. As mentioned above, LCs with the nanostructured Al surface can achieve colors tuning over the entire visible range. The mechanical chameleon is demonstrated and fabricated based on the integrated Au/Ag core-shell nanodome array, and the dynamically tunable surface color is realized experimentally. The electrochromic approach, mechanical stretching with metasurfaces or stress-releasable material, can also achieve a full visible tuning range. Besides, the combination of assembled colloidal microspheres and real-time response material provides an effective approach to prepare low-cost and large-scale structural colors. Moreover, there are many other proper approaches to dynamically tune the structural colors, such as metasurfaces with catalytic magnesium and photon doping.[168–171]

SUMMARY AND OUTLOOK

Collectively, we addressed nanostructures generating colors and the dynamically tunable colors along with their applications in this review. Many works related to artificial structural colors have been reported recently, which are generated by multilayer films, photonic crystals, and metasurfaces. The multilayer films can create high-efficiency colors and be simply fabricated by the deposition process. They can be integrated to achieve high-resolution images. Bionics metasurfaces and photonic crystals are widely investigated. Researchers have obtained high-resolution, robust, and vivid color filters, which are inspired by microstructures of natural creatures. Grating structure based on GMR provides a narrow bandwidth resonance with high efficiency, and a high degree of optical tunability, while it needs tens of periods to achieve adequate performance and restrict its spatial resolution. As for the assembly of colloidal crystals, it is an easy way to generate low-cost and large-scale structural colors, which mainly benefits from the simple process. The metallic metasurface generating colors with SPR and LSPR have broadband visible spectra and low efficiency due to the loss of material. In contrast, all-dielectric structures based on Mie resonance or Fano resonance show a narrow resonance band and high efficiency, which can be used in fields like thermophotovoltaics and photovoltaics. Disordered structures based on dielectric or metal NPs are also a major way to realize structural colors. Besides, the colors generated by artificial structures can be dynamically tuned by reconfigurable LCs, electrochromic and plasmonic modulation, mechanical stretching, and so on. It is worth noting that artificial structural colors can even have multiple functions besides decoration, such as solar energy absorbing, anti-counterfeiting, information encryption, and so on, which are superior to conventional pigments and dyes. Table 1 summarizes the main structural colors, as well as their principles, properties, and challenges.

Taken together, although significant progress in structural colors has been made in the last decades, there is still huge developmental potential to provide practical applications. For instance, the main challenges to using structural colors for high-end display and high-resolution printing include large-scale production, high color vibrancy, and angular independence. Researchers have worked to solve these problems, and there is fabricated production with suitable property in each aspect. However, highly precise

nanofabrication processes, like EBL or FIB, are required, which dramatically increase the manufacturing cost and make it hard to be practically applied in the market. Therefore, approaches to fabricate large-scale and low-cost structural color processes, like nanoimprint lithography, injection molding, and self-assembly techniques, have been widely developed. However, there is still room to develop dynamically tunable structural color for large-scale industrial preparation. Dynamically tunable structural colors from assembled colloidal crystals and films enable large-scale and low-cost preparation, while they cannot be used in fields that request high resolution. Metasurface structures can also realize dynamically tunable structural colors by combining with LCs, electrochromic solution, phase change material, and so on. These approaches can generate high-resolution dynamically tunable structural colors from periodic subwavelength nanostructure, which need high-cost and time-consuming fabrication processes. Only inch-level structural colors can be fabricated by current micro-nano process equipment, which is far from the pigments-and-dyes approaches. Moreover, the combination of metasurfaces and dynamically tunable materials makes the fabrication process more complicated, restricting the product yield. It restricts the large-scale fabrication of dynamically tunable structural color based on metasurfaces. Therefore, the development of fast and highly efficient micro-nano fabrication processes, such as nano-imprinting, is the key to achieve large-scale fabrication of high-resolution dynamically tunable structural colors.

We believe that inexpensive structural colors with high resolution, durable surfaces, and high color vibrancy can be realized in the future. Moreover, the real-time tunable structures will be used in fields like product design and art layout. Some structures can be designed to have more functions, such as colorful solar energy absorbers, metasurfaces for holograms, and so on. Compared with conventional dyes and pigments, structural colors hold advantages of long-term durability, environmentally friendliness, resolution beyond diffraction limits, dynamic tunability, and multi-functions. Although it is hard to completely replace the widely used dyes and pigments, structural colors possessing excellent properties open a prospective and bright future in many fields, including anti-counterfeit labels, optical data storage, and surface decoration. It will be a new generation of technology to provide a colorful and environmentally friendly world.

REFERENCES

1. Hook. (1665). Micrographia: Or Some Physiological Descriptions of Minute Bodies Made by Magnifying Glasses with Observations and Inquiries Thereupon (London: Royal Society).
2. Newton, I. (1952). Opticks, or, A Treatise of the Reflections, Refractions, Inflections and Colours of Light (Repr. from the 4th ed.) (American Journal of Ophthalmology), p. 66.
3. Tayeb, G., Gralak, B., and Enoch, S. (2003). Structural colors in nature and butterfly-wing modelling. Opt. Photon. News ***14***, 38.
4. Zi, J., Yu, X.D., Li, Y.Z., et al. (2003). Coloration strategies in peacock feathers. Proc. Natl. Acad. Sci. U S A ***100***, 12576–12578.
5. Chung, K., Yu, S., Heo, C.J., et al. (2012). Flexible, angle-independent, structural color reflectors inspired by Morpho butterfly wings. Adv. Mater. ***24***, 2375–2379.
6. Kinoshita, S., Yoshioka, S., and Kawagoe, K. (2002). Mechanisms of structural colour in the Morpho butterfly: cooperation of regularity and irregularity in an iridescent scale. Proc. R. Soc. Lond. Ser. B Biol. Sci. ***269***, 1417–1421.
7. Prum, R.O., Quinn, T., and Torres, R.H. (2006). Anatomically diverse butterfly scales all produce structural colours by coherent scattering. J. Exp. Biol. ***209***, 748–765.
8. Zhao, Y., Xie, Z., Gu, H., et al. (2012). Bio-inspired variable structural color materials. Chem. Soc. Rev. ***41***, 3297–3317.
9. Teyssier, J., Saenko, S.V., van der Marel, D., et al. (2015). Photonic crystals cause active colour change in chameleons. Nat. Commun. ***6***, 6368.
10. Shang, L., Zhang, W., Xu, K., et al. (2019). Bio-inspired intelligent structural color materials. Mater. Horiz. ***6***, 945–958.
11. Fu, F.F., Shang, L.R., Chen, Z.Y., et al. (2018). Bioinspired living structural color hydrogels. Sci. Robot. ***3***, 8.
12. Diest, K., Dionne, J.A., Spain, M., et al. (2009). Tunable color filters based on metal-insulator-metal resonators. Nano Lett. ***9***, 2579–2583.
13. Ellenbogen, T., Seo, K., and Crozier, K.B. (2012). Chromatic plasmonic polarizers for active visible color filtering and polarimetry. Nano Lett. ***12***, 1026–1031.
14. Fudouzi, H., and Xia, Y.N. (2003). Photonic papers and inks: color writing with colorless materials. Adv. Mater. ***15***, 892.
15. Jiang, X., Gu, Q., Wang, F., et al. (2013). Fabrication of coaxial plasmonic crystals by focused ion beam milling and electron-beam lithography. Mater. Lett. ***100***, 192–194.
16. Kaplan, A.F., Xu, T., and Guo, L.J. (2011). High efficiency resonance-based spectrum filters with tunable transmission bandwidth fabricated using nanoimprint lithography. Appl. Phys. Lett. ***99***, 143111.
17. Yokogawa, S., Burgos, S.P., and Atwater, H.A. (2012). Plasmonic color filters for CMOS image sensor applications. Nano Lett. ***12***, 4349–4354.
18. Arsenault, A.C., Puzzo, D.P., Manners, I., et al. (2007). Photonic-crystal full-colour displays. Nat. Photon. ***1***, 468–472.
19. Si, G., Zhao, Y., Lv, J., et al. (2013). Reflective plasmonic color filters based on lithographically patterned silver nanorod arrays. Nanoscale ***5***, 6243–6248.
20. Burgos, S.P., Yokogawa, S., and Atwater, H.A. (2013). Color imaging via nearest neighbor hole coupling in plasmonic color filters integrated onto a complementary metal-oxide semiconductor image sensor. ACS Nano ***7***, 10038–10047.
21. Le Perchec, J., Desieres, Y., Rochat, N., et al. (2012). Subwavelength optical absorber with an integrated photon sorter. Appl. Phys. Lett. ***100***, 113305.
22. Lien, A., Cai, C., John, R.A., et al. (2001). 16.3 " QSXGA high resolution wide viewing angle TFT-LCDs based on ridge and fringe-field structures. Displays ***22***, 9–14.
23. Roberts, A.S., Pors, A., Albrektsen, O., et al. (2014). Subwavelength plasmonic color printing protected for ambient use. Nano Lett. ***14***, 783–787.
24. Si, G., Zhao, Y., Liu, H., et al. (2011). Annular aperture array based color filter. Appl. Phys. Lett. ***99***, 033105.
25. Bhushan, B. (2017). Springer Handbook of Nanotechnology, ***73***, 4th edition (Tribology & Lubrication Technology), p. 78.
26. Shalaev, V.M. (2007). Optical negative-index metamaterials. Nat. Photon. ***1***, 41–48.
27. Do, Y.S., Park, J.H., Hwang, B.Y., et al. (2013). Plasmonic color filter and its fabrication for large-area applications. Adv. Opt. Mater. ***1***, 133–138.
28. Si, G., Jiang, X., Lv, J., et al. (2014). Fabrication and characterization of well-aligned plasmonic nanopillars with ultrasmall separations. Nanoscale Res. Lett. ***9***, 299.
29. Si, G., Wang, Q., Lv, J., et al. (2014). Interference lithography patterned large area plasmonic nanodisks for infrared detection. Mater. Lett. ***128***, 373–375.
30. Shen, Y.C., Rinnerbauer, V., Wang, I., et al. (2015). Structural colors from Fano resonances. ACS Photon. ***2***, 27–32.
31. Si, G., Danner, A.J., Teo, S.L., et al. (2011). Photonic crystal structures with ultrahigh aspect ratio in lithium niobate fabricated by focused ion beam milling. J. Vac. Sci. Technol. B Nanotechnol. Microelectron. Mater. Process. Meas. Phenomena ***29***, 021205.
32. Clausen, J.S., Hojlund-Nielsen, E., Christiansen, A.B., et al. (2014). Plasmonic metasurfaces for coloration of plastic consumer products. Nano Lett. ***14***, 4499–4504.
33. Shalaev, M.I., Sun, J., Tsukernik, A., et al. (2015). High-efficiency all-dielectric metasurfaces for ultracompact beam manipulation in transmission mode. Nano Lett. ***15***, 6261–6266.
34. Meinzer, N., Barnes, W.L., and Hooper, I.R. (2014). Plasmonic meta-atoms and metasurfaces. Nat. Photon. ***8***, 889–898.
35. Kuznetsov, A.I., Miroshnichenko, A.E., Brongersma, M.L., et al. (2016). Optically resonant dielectric nanostructures. Science ***354***, aag2472.
36. Karimi, E., Schulz, S.A., De Leon, I., et al. (2014). Generating optical orbital angular momentum at visible wavelengths using a plasmonic metasurface. Light Sci. Appl. ***3***, 4.
37. Genevet, P., Capasso, F., Aieta, F., et al. (2017). Recent advances in planar optics: from plasmonic to dielectric metasurfaces. Optica ***4***, 139–152.
38. Zhao, J., Yu, X., Zhou, K., et al. (2019). Wide-gamut and polarization-independent structural color at optical sub-diffraction-limit spatial resolution based on uncoupled LSPPs. Nanoscale Res. Lett. ***14***, 214.
39. Wu, Y.-K.R., Hollowell, A.E., Zhang, C., et al. (2013). Angle-insensitive structural colours based on metallic nanocavities and coloured pixels beyond the diffraction limit. Sci. Rep. ***3***, 1194.
40. Tan, S.J., Zhang, L., Zhu, D., et al. (2014). Plasmonic color palettes for photorealistic printing with aluminum nanostructures. Nano Lett. ***14***, 4023–4029.
41. Kumar, K., Duan, H., Hegde, R.S., et al. (2012). Printing colour at the optical diffraction limit. Nat. Nanotechnol. ***7***, 557–561.
42. Cho, E.-H., Kim, H.-S., Sohn, J.-S., et al. (2010). Nanoimprinted photonic crystal color filters for solar-powered reflective displays. Opt. Express ***18***, 27712–27722.
43. Zhao, Y., Zhao, Y., Hu, S., et al. (2017). Artificial structural color pixels: a review. Materials (Basel) ***10***.
44. Cao, L., Fan, P., Barnard, E.S., et al. (2010). Tuning the color of silicon nanostructures. Nano Lett. ***10***, 2649–2654.
45. Nagasaki, Y., Suzuki, M., and Takahara, J. (2017). All-dielectric dual-color pixel with subwavelength resolution. Nano Lett. ***17***, 7500–7506.
46. Naik, G.V., Shalaev, V.M., and Boltasseva, A. (2013). Alternative plasmonic materials: beyond gold and silver. Adv. Mater. ***25***, 3264–3294.
47. Proust, J., Bedu, F., Gallas, B., et al. (2016). All-dielectric colored metasurfaces with silicon Mie resonators. ACS Nano ***10***, 7761–7767.
48. Sun, S., Zhou, Z., Zhang, C., et al. (2017). All-dielectric full-color printing with TiO2 metasurfaces. ACS Nano ***11***, 4445–4452.

49. Goh, X.M., Ng, R.J.H., Wang, S.H., et al. (2016). Comparative study of plasmonic colors from all-metal structures of posts and pits. ACS Photon. ***3***, 1000–1009.
50. Ng, R.J.H., Goh, X.M., and Yang, J.K.W. (2015). All-metal nanostructured substrates as subtractive color reflectors with near-perfect absorptance. Opt. Express ***23***, 32597–32605.
51. Mihi, A., Ocana, M., and Miguez, H. (2006). Oriented colloidal-crystal thin films by spin-coating microspheres dispersed in volatile media. Adv. Mater. ***18***, 2244.
52. Gao, Z., Huang, C., Yang, D., et al. (2018). Dual-mode multicolored photonic crystal patterns enabled by ultraviolet-responsive core-shell colloidal spheres. Dyes Pigm. ***148***, 108–117.
53. Wang, Y., Shang, L., Bian, F., et al. (2019). Hollow colloid assembled photonic crystal clusters as suspension barcodes for multiplex bioassays. Small ***15***, 1900056.
54. Shang, L., Cheng, Y., and Zhao, Y. (2017). Emerging droplet microfluidics. Chem. Rev. ***117***, 7964–8040.
55. Qin, M., Huang, Y., Li, Y., et al. (2016). A rainbow structural-color chip for multisaccharide recognition. Angew. Chem. Int. Ed. ***55***, 6911–6914.
56. Chen, J., Xu, L., Yang, M., et al. (2019). Highly stretchable photonic crystal hydrogels for a sensitive mechanochromic sensor and direct ink writing. Chem. Mater. ***31***, 8918–8926.
57. Chen, F., Wang, S.-W., Liu, X., et al. (2016). Colorful solar selective absorber integrated with different colored units. Opt. Express ***24***, A92–A103.
58. Chen, F., Wang, S.-W., Liu, X., et al. (2015). High performance colored selective absorbers for architecturally integrated solar applications. J. Mater. Chem. A ***3***, 7353–7360.
59. Nam, H., Song, K., Ha, D., et al. (2016). Inkjet printing based mono-layered photonic crystal patterning for anti-counterfeiting structural colors. Sci. Rep. ***6***, 30885.
60. Cui, Y., Hegde, R.S., Phang, I.Y., et al. (2014). Encoding molecular information in plasmonic nanostructures for anti-counterfeiting applications. Nanoscale ***6***, 282–288.
61. Yao, J., Zhang, C., Liu, H., et al. (2012). Selective appearance of several laser-induced periodic surface structure patterns on a metal surface using structural colors produced by femtosecond laser pulses. Appl. Surf. Sci. ***258***, 7625–7632.
62. Tian, W., Zhang, J., Yu, J., et al. (2018). Phototunable full-color emission of cellulose-based dynamic fluorescent materials. Adv. Funct. Mater. ***28***, 1703548.
63. Song, M., Li, X., Pu, M., et al. (2018). Color display and encryption with a plasmonic polarizing metamirror. Nanophotonics ***7***, 323–331.
64. Gao, Y., Huang, C., Hao, C., et al. (2018). Lead halide perovskite nanostructures for dynamic color display. ACS Nano ***12***, 8847–8854.
65. Abuturab, M.R. (2012). Color image security system using double random-structured phase encoding in gyrator transform domain. Appl. Opt. ***51***, 3006–3016.
66. Yang, Z., Chen, Y., Zhou, Y., et al. (2017). Microscopic interference full-color printing using grayscale-patterned Fabry-Perot resonance cavities. Adv. Opt. Mater. ***5***, 1700029.
67. Mao, P., Liu, C., Song, F., et al. (2020). Manipulating disordered plasmonic systems by external cavity with transition from broadband absorption to reconfigurable reflection. Nat. Commun. ***11***, 1538.
68. Vigneron, J.-P., and Simonis, P. (2010). Structural colours. In Advances in Insect Physiology (Elsevier), pp. 181–218.
69. Kinoshita, S., Yoshioka, S., and Miyazaki, J. (2008). Physics of structural colors. Rep. Prog. Phys. ***71***, 076401.
70. Ito, M.M., Gibbons, A.H., Qin, D.T., et al. (2019). Structural colour using organized microfibrillation in glassy polymer films. Nature ***570***, 363.
71. Yang, Z., Zhou, Y., Chen, Y., et al. (2016). Reflective color filters and monolithic color printing based on asymmetric Fabry-Perot cavities using nickel as a broadband absorber. Adv. Opt. Mater. ***4***, 1196–1202.
72. Han, J.H., Kim, D.-Y., Kim, D., et al. (2016). Highly conductive and flexible color filter electrode using multilayer film structure. Sci. Rep. ***6***, 29341.
73. Guo, J., Huard, C.M., Yang, Y., et al. (2014). ITO-free, compact, color liquid crystal devices using integrated structural color filters and graphene electrodes. Adv. Opt. Mater. ***2***, 435–441.
74. Yang, C., Mao, K., Shen, W., et al. (2016). Tunable, omnidirectional structural color on reflection based on metal-SiOx-metal structure. Appl. Phys. Lett. ***109***, 241104.
75. Li, Z., Butun, S., and Aydin, K. (2015). Large-area, lithography-free super absorbers and color filters at visible frequencies using ultrathin metallic films. ACS Photon. ***2***, 183–188.
76. Wang, Y., Zheng, M., Ruan, Q., et al. (2018). Stepwise-nanocavity-assisted transmissive color filter array microprints. Research (Wash. D.C.) ***2018***, 8109054.
77. Lee, K.-T., Lee, J.Y., Seo, S., et al. (2014). Colored ultrathin hybrid photovoltaics with high quantum efficiency. Light Sci. Appl. ***3***, e215–e215.
78. Wang, S.W., Liu, D.Q., Lin, B., et al. (2004). Realization of integrated narrow bandpass filters in the infrared region. Int. J. Infrared Millimeter Waves ***25***, 1677–1683.
79. Wang, S.W., Chen, X.S., Lu, W., et al. (2006). Integrated optical filter arrays fabricated by using the combinatorial etching technique. Opt. Lett. ***31***, 332–334.
80. Wang, S.W., Liu, D., Lin, B., et al. (2006). 16 x 1 integrated filter array in the MIR region prepared by using a combinatorial etching technique. Appl. Phys. B Lasers Opt. ***82***, 637–641.
81. Wang, S.W., Li, M., Xia, C.S., et al. (2007). 128 channels of integrated filter array rapidly fabricated by using the combinatorial deposition technique. Appl. Phys. B Lasers Opt. ***88***, 281–284.
82. Wang, S.-W., Chen, X., Lu, W., et al. (2007). Fractal independently tunable multichannel filters. Appl. Phys. Lett. ***90***, 211113.
83. Wang, S.-W., Xia, C., Chen, X., et al. (2007). Concept of a high-resolution miniature spectrometer using an integrated filter array. Opt. Lett. ***32***, 632–634.
84. Xuan, Z.Y., Zhi, Y., Wang, S.W., et al. (2019). Rapid and precise wavelength determination approach based on visually patterned integrated narrow bandpass filters. IEEE Photon. J ***11***, 1–7.
85. Ji, C., Lee, K.-T., Xu, T., et al. (2017). Engineering light at the nanoscale: structural color filters and broadband perfect absorbers. Adv. Opt. Mater. ***5***, 1700368.
86. Lee, K.-T., Seo, S., Lee, J.Y., et al. (2014). Ultrathin metal-semiconductor-metal resonator for angle invariant visible band transmission filters. Appl. Phys. Lett. ***104***, 231112.
87. Yu, Y., Wen, L., Song, S., et al. (2014). Transmissive/reflective structural color filters: theory and applications. J. Nanomater. 212637.
88. Park, C.-S., Shrestha, V.R., Lee, S.-S., et al. (2015). Omnidirectional color filters capitalizing on a nano-resonator of Ag-TiO2-Ag integrated with a phase compensating dielectric overlay. Sci. Rep. ***5***, 8467.
89. Kats, M.A., Blanchard, R., Genevet, P., et al. (2013). Nanometre optical coatings based on strong interference effects in highly absorbing media. Nat. Mater. ***12***, 20–24.
90. Kats, M.A., and Capasso, F. (2016). Optical absorbers based on strong interference in ultra-thin films. Laser Photon. Rev. ***10***, 735–749.
91. Zhao, J., Qiu, M., Yu, X., et al. (2019). Defining deep-subwavelength-resolution, wide-color-gamut, and large-viewing-angle flexible subtractive colors with an ultrathin asymmetric Fabry-Perot lossy cavity. Adv. Opt. Mater. ***7***, 1900646.
92. Lee, K.T., Seo, S., Lee, J.Y., et al. (2014). Strong resonance effect in a lossy medium-based optical cavity for angle robust spectrum filters. Adv. Mater. ***26***, 6324–6328.
93. Srinivasarao, M. (1999). Nano-optics in the biological world: beetles, butterflies, birds, and moths. Chem. Rev. ***99***, 1935–1961.
94. Kolle, M., Salgard-Cunha, P.M., Scherer, M.R.J., et al. (2010). Mimicking the colourful wing scale structure of the Papilio blumei butterfly. Nat. Nanotechnol. ***5***, 511–515.
95. Seo, K., Wober, M., Steinvurzel, P., et al. (2011). Multicolored vertical silicon nanowires. Nano Lett. ***11***, 1851–1856.
96. Sun, S., Zhou, Z., Duan, Z., et al. (2017). All-dielectric metasurface for polarization-insensitive color printing. In Conference on Lasers and Electro-Optics (CLEO).
97. Flauraud, V., Reyes, M., Paniagua-Dominguez, R., et al. (2017). Silicon nanostructures for bright field full color prints. ACS Photon. ***4***, 1913–1919.
98. Kim, H., Ge, J.P., Kim, J., et al. (2009). Structural colour printing using a magnetically tunable and lithographically fixable photonic crystal. Nat. Photon. ***3***, 534–540.
99. Huo, P., Song, M., Zhu, W., et al. (2020). Photorealistic full-color nanopainting enabled by a low-loss metasurface. Optica ***7***, 1171–1172.
100. Wang, H., Liu, Y., Chen, Z., et al. (2020). Anisotropic structural color particles from colloidal phase separation. Sci. Adv. ***6***, eaay1438.
101. Wang, Y., Shang, L., Chen, G., et al. (2020). Bioinspired structural color patch with anisotropic surface adhesion. Sci. Adv. ***6***, eaax8258.
102. Shen, Z., Shi, L., You, B., et al. (2012). Large-scale fabrication of three-dimensional ordered polymer films with strong structure colors and robust mechanical properties. J. Mater. Chem. ***22***, 8069–8075.
103. Shen, Z.H., Yang, Y.Y., Lu, F.Z., et al. (2012). Self-assembly of binary particles and application as structural colors. Polym. Chem. ***3***, 2495–2501.
104. Li, F., Tang, B., and Zhang, S. (2017). Iridescent structural colors from self-assembled polymer opal of polythiourethane microspheres. Dyes Pigm. ***142***, 371–378.
105. Huang, C., Zhang, H., Yang, S., et al. (2020). Controllable structural colored screen for real-time display via near-infrared light. ACS Appl. Mater. Interfaces ***12***, 20867–20873.
106. Zhao, R., Huang, L., and Wang, Y. (2020). Recent advances in multi-dimensional metasurfaces holographic technologies. PhotoniX ***1***, 20.
107. Quaranta, G., Basset, G., Martin, O.J.F., et al. (2018). Recent advances in resonant waveguide gratings. Laser Photon. Rev. ***12***, 1800017.
108. Tibuleac, S., and Magnusson, R. (1997). Reflection and transmission guided-mode resonance filters. J. Opt. Soc. Am. A Opt. Image Sci. Vis. ***14***, 1617–1626.
109. Uddin, M.J., Khaleque, T., and Magnusson, R. (2014). Guided-mode resonant polarization-controlled tunable color filters. Opt. Express ***22***, 12307–12315.
110. Liu, Z.S., Tibuleac, S., Shin, D., et al. (1998). High-efficiency guided-mode resonance filter. Opt. Lett. ***23***, 1556–1558.
111. Wang, S.S., and Magnusson, R. (1993). Theory and applications of guided-mode resonance filters. Appl. Opt. ***32***, 2606–2613.
112. Yoon, Y.-T., Lee, H.-S., Lee, S.-S., et al. (2008). Color filter incorporating a subwavelength patterned grating in poly silicon. Opt. Express ***16***, 2374–2380.
113. Kanamori, Y., Katsube, H., Furuta, T., et al. (2009). Design and fabrication of structural color filters with polymer-based guided-mode resonant gratings by nanoimprint lithography. Jpn. J. Appl. Phys. ***48***, 06FH04.

114. Park, C.H., Yoon, Y.T., Shrestha, V.R., et al. (2013). Electrically tunable color filter based on a polarization-tailored nano-photonic dichroic resonator featuring an asymmetric subwavelength grating. Opt. Express ***21***, 28783–28793.
115. Zhu, X., Yan, W., Levy, U., et al. (2017). Resonant laser printing of structural colors on high-index dielectric metasurfaces. Sci. Adv. ***3***, e1602487.
116. Liu, T., VanSaders, B., Glotzer, S.C., et al. (2020). Effect of defective microstructure and film thickness on the reflective structural color of self-assembled colloidal crystals. ACS Appl. Mater. Interfaces ***12***, 9842–9850.
117. Fan, S.H., and Joannopoulos, J.D. (2002). Analysis of guided resonances in photonic crystal slabs. Phys. Rev. B ***65***, 235112.
118. Schattenburg, M.L., Aucoin, R.J., and Fleming, R.C. (1995). Optically matched trilevel resist process for nanostructure fabrication. J. Vac. Sci. Technol. B ***13***, 3007–3011.
119. Xia, Y.N., Gates, B., Yin, Y.D., et al. (2000). Monodispersed colloidal spheres: old materials with new applications. Adv. Mater. ***12***, 693–713.
120. Vlasov, Y.A., Bo, X.Z., Sturm, J.C., et al. (2001). On-chip natural assembly of silicon photonic bandgap crystals. Nature ***414***, 289–293.
121. Wang, D.Y., Caruso, R.A., and Caruso, F. (2001). Synthesis of macroporous titania and inorganic composite materials from coated colloidal spheres - a novel route to tune pore morphology. Chem. Mater. ***13***, 364–371.
122. Wong, S., Kitaev, V., and Ozin, G.A. (2003). Colloidal crystal films: advances in universality and perfection. J. Am. Chem. Soc. ***125***, 15589–15598.
123. Duan, H., Hu, H., Kumar, K., et al. (2011). Direct and reliable patterning of plasmonic nanostructures with sub-10-nm gaps. ACS Nano ***5***, 7593–7600.
124. Dean, N. (2015). Colouring at the nanoscale. Nat. Nanotechnol. ***10***, 15–16.
125. Zhu, X.L., Vannahme, C., Hojlund-Nielsen, E., et al. (2016). Plasmonic colour laser printing. Nat. Nanotechnol. ***11***, 325.
126. Yue, W., Gao, S., Lee, S.S., et al. (2016). Subtractive color filters based on a silicon-aluminum hybrid-nanodisk metasurface enabling enhanced color purity. Sci. Rep. ***6***, 29756.
127. James, T.D., Mulvaney, P., and Roberts, A. (2016). The plasmonic pixel: large area, wide gamut color reproduction using aluminum nanostructures. Nano Lett. ***16***, 3817–3823.
128. Hojlund-Nielsen, E., Clausen, J., Makela, T., et al. (2016). Plasmonic colors: toward mass production of metasurfaces. Adv. Mater. Technol. ***1***, 1600054.
129. Heydari, E., Sperling, J.R., Neale, S.L., et al. (2017). Plasmonic color filters as dual-state nanopixels for high-density microimage encoding. Adv. Funct. Mater. ***27***, 1701866.
130. Chen, Z.Q., Li, P., Zhang, S., et al. (2019). Enhanced extraordinary optical transmission and refractive-index sensing sensitivity in tapered plasmonic nanohole arrays. Nanotechnology ***30***, 335201.
131. Genet, C., and Ebbesen, T.W. (2007). Light in tiny holes. Nature ***445***, 39–46.
132. Cheng, F., Gao, J., Luk, T.S., et al. (2015). Structural color printing based on plasmonic metasurfaces of perfect light absorption. Sci. Rep. ***5***, 11045.
133. Goh, X.M., Zheng, Y., Tan, S.J., et al. (2014). Three-dimensional plasmonic stereoscopic prints in full colour. Nat. Commun. ***5***, 5361.
134. Joo, W.-J., Kyoung, J., Esfandyarpour, M., et al. (2020). Metasurface-driven OLED displays beyond 10,000 pixels per inch. Science ***370***, 459–463.
135. Lee, Y.-C., Huang, C.-F., Chang, J.-Y., et al. (2008). Enhanced light trapping based on guided mode resonance effect for thin-film silicon solar cells with two filling-factor gratings. Opt. Express ***16***, 7969–7975.
136. Ghaemi, H.F., Thio, T., Grupp, D.E., et al. (1998). Surface plasmons enhance optical transmission through subwavelength holes. Phys. Rev. B ***58***, 6779–6782.
137. Koirala, I., Shrestha, V.R., Park, C.-S., et al. (2017). Polarization-controlled broad color palette based on an ultrathin one-dimensional resonant grating structure. Sci. Rep. ***7***, 40073.
138. Kristensen, A., Yang, J.K.W., Bozhevolnyi, S.I., et al. (2017). Plasmonic colour generation. Nat. Rev. Mater. ***2***, 16088.
139. Cho, E.-H., Kim, H.-S., Cheong, B.-H., et al. (2009). Two-dimensional photonic crystal color filter development. Opt. Express ***17***, 8621–8629.
140. Park, C.-H., Yoon, Y.-T., and Lee, S.-S. (2012). Polarization-independent visible wavelength filter incorporating a symmetric metal-dielectric resonant structure. Opt. Express ***20***, 23769–23777.
141. Shrestha, V.R., Lee, S.S., Kim, E.S., et al. (2015). Polarization-tuned dynamic color filters incorporating a dielectric-loaded aluminum nanowire array. Sci. Rep. ***5***, 12450.
142. Boye, R.R., and Kostuk, R.K. (2000). Investigation of the effect of finite grating size on the performance of guided-mode resonance filters. Appl. Opt. ***39***, 3649–3653.
143. Zheng, G., Cong, J., Xu, L., et al. (2014). Angle-insensitive and narrow band grating filter with a gradient-index layer. Opt. Lett. ***39***, 5929–5932.
144. Ye, Y., Shao, R., Zhou, Y., et al. (2012). Wide-angle transmissive filter based on a guided-mode resonant grating. Appl. Opt. ***51***, 5785–5790.
145. Xu, B., Zhang, D., Huang, Y., et al. (2014). Real-time angular sensitivity compensation of guided-mode resonance filter. IEEE Photon. Technol. Lett. ***26***, 231–234.
146. Buet, X., Daran, E., Belharet, D., et al. (2012). High angular tolerance and reflectivity with narrow bandwidth cavity-resonator-integrated guided-mode resonance filter. Opt. Express ***20***, 9322–9327.
147. Sentenac, A., and Fehrembach, A.L. (2005). Angular tolerant resonant grating filters under oblique incidence. J. Opt. Soc. Am. A Opt. Image Sci. Vis. ***22***, 475–480.
148. Sato, A., Iwai, N., and Sato, M. (2010). Large incident angle tolerance of guided-mode resonant gratings by light coupling via waveguide end faces. J. Opt. Soc. Am. A Opt. Image Sci. Vis. ***27***, 1671–1678.
149. Shah, Y.D., Connolly, P.W.R., Grant, J.P., et al. (2020). Ultralow-light-level color image reconstruction using high-efficiency plasmonic metasurface mosaic filters. Optica ***7***, 632–639.
150. Si, G., Zhao, Y., Leong, E.S.P., et al. (2014). Liquid-crystal-enabled active plasmonics: a review. Materials ***7***, 1296–1317.
151. Bartholomew, R., Williams, C., Khan, A., et al. (2017). Plasmonic nanohole electrodes for active color tunable liquid crystal transmissive pixels. Opt. Lett. ***42***, 2810–2813.
152. Liu, Y.J., Si, G.Y., Leong, E.S.P., et al. (2012). Light-driven plasmonic color filters by overlaying photoresponsive liquid crystals on gold annular aperture arrays. Adv. Mater. ***24***, OP131–OP135.
153. Olson, J., Manjavacas, A., Basu, T., et al. (2016). High chromaticity aluminum plasmonic pixels for active liquid crystal displays. ACS Nano ***10***, 1108–1117.
154. Franklin, D., Chen, Y., Vazquez-Guardado, A., et al. (2015). Polarization-independent actively tunable colour generation on imprinted plasmonic surfaces. Nat. Commun. ***6***, 7337.
155. Franklin, D., Frank, R., Wu, S.-T., et al. (2017). Actively addressed single pixel full-colour plasmonic display. Nat. Commun. ***8***, 15209.
156. Liu, Q., Yuan, Y., and Smalyukh, I.I. (2014). Electrically and optically tunable plasmonic guest-host liquid crystals with long-range ordered nanoparticles. Nano Lett. ***14***, 4071–4077.
157. Li, H., Xu, S., Wang, H., et al. (2014). Active-tuned plasmonic angle modulator of light beams for potential application of 3D display. ACS Photon. ***1***, 677–682.
158. Dickson, W., Wurtz, G.A., Evans, P.R., et al. (2008). Electronically controlled surface plasmon dispersion and optical transmission through metallic hole arrays using liquid crystal. Nano Lett. ***8***, 281–286.
159. Wang, G.P., Chen, X.C., Liu, S., et al. (2016). Mechanical chameleon through dynamic real time-plasmonic tuning. ACS Nano ***10***, 1788–1794.
160. Somani, P.R., and Radhakrishnan, S. (2003). Electrochromic materials and devices: present and future. Mater. Chem. Phys. ***77***, 117–133.
161. Rosseinsky, D.R., and Mortimer, R.J. (2001). Electrochromic systems and the prospects for devices. Adv. Mater. ***13***, 783.
162. Mortimer, R.J., Dyer, A.L., and Reynolds, J.R. (2006). Electrochromic organic and polymeric materials for display applications. Displays ***27***, 2–18.
163. Argun, A.A., Aubert, P.H., Thompson, B.C., et al. (2004). Multicolored electrochromism polymers: structures and devices. Chem. Mater. ***16***, 4401–4412.
164. Xu, T., Walter, E.C., Agrawal, A., et al. (2016). High-contrast and fast electrochromic switching enabled by plasmonics. Nat. Commun. ***7***, 10479.
165. Liu, C., Fan, Z., Tan, Y., et al. (2020). Tunable structural color patterns based on the visible-light-responsive dynamic diselenide metathesis. Adv. Mater. ***32***, e1907569.
166. Kumagai, H., Fujie, T., Sawada, K., et al. (2020). Stretchable and high-adhesive plasmonic metasheet using Al subwavelength grating embedded in an elastomer nanosheet. Adv. Opt. Mater. 1902074.
167. Tseng, M.L., Yang, J., Semmlinger, M., et al. (2017). Two-dimensional active tuning of an aluminum plasmonic array for full-spectrum response. Nano Lett. ***17***, 6034–6039.
168. Sautter, J., Staude, I., Decker, M., et al. (2015). Active tuning of all-dielectric metasurfaces. ACS Nano ***9***, 4308–4315.
169. Sterl, F., Strohfeldt, N., Walter, R., et al. (2015). Magnesium as novel material for active plasmonics in the visible wavelength range. Nano Lett. ***15***, 7949–7955.
170. Li, J., Chen, Y., Hu, Y., et al. (2020). Magnesium-based metasurfaces for dual-function switching between dynamic holography and dynamic color display. ACS Nano, 7892–7898.
171. Wu, H., Zhang, B., Liang, H., et al. (2020). Distance effect of Ni-Pt dual sites for active hydrogen transfer in tandem reaction. Innovation ***1***, 100029.

ACKNOWLEDGMENTS

This work was funded by the National Natural Science Foundation of China (NSFC) (11874376), Shanghai Science and Technology Foundations (18590712600, 18DZ2282200, 19DZ2293400, 19ZR1465900), Shanghai Municipal Science and Technology Major Project (2019SHZDZX01), and the Chinese Academy of Sciences President's International Fellowship Initiative (2020VTA0009, 2020PT0020, 2021PT0007).

AUTHOR CONTRIBUTIONS

Z.X. and J.L. contributed equally to writing the manuscript. Q.L., F.Y., and W.L. helped writing the manuscript. S.W. supervised, organized and revised the manuscript. All authors read and approved the final manuscript.

DECLARATION OF INTERESTS

The authors declare that they have no conflicts of interest.

LEAD CONTACT WEBSITES

https://orcid.org/0000-0002-6624-2016